HEATSTORE
Monitoring results for the Geneva HT-ATES case-study

Prepared by: Luca Guglielmetti (UniGe)
Nicolas Houlié (Nicolas Houlie Geologie GmbH)
Carole Nawratil de Bono, Francois Martin, Jerome Coudroit (SIG)

Checked by: Peter Oerlemans (IF Technology)
Approved by: Holger Cremer (TNO)

Please cite this report as: Guglielmetti et al. 2021: HEATSTORE D5.2: Monitoring results for the Geneva HT-ATES case-study. HEATSTORE project report, GEOTHERMICA – ERA NET Cofund Geothermal. 33 pp.

This report is one of the documents delivered in the HEATSTORE project deliverable number D5.2.

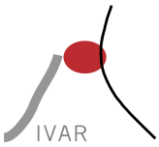

HEATSTORE (170153-4401) is one of nine projects under the GEOTHERMICA – ERA NET Cofund aimed at accelerating the uptake of geothermal energy by 1) advancing and integrating different types of underground thermal energy storage (UTES) in the energy system, 2) providing a means to maximise geothermal heat production and optimise the business case of geothermal heat production doublets, 3) addressing technical, economic, environmental, regulatory and policy aspects that are necessary to support efficient and cost-effective deployment of UTES technologies in Europe.

This project has been subsidized through the ERANET cofund GEOTHERMICA (Project n. 731117), from the European Commission, RVO (the Netherlands), DETEC (Switzerland), FZJ-PtJ (Germany), ADEME (France), EUDP (Denmark), Rannis (Iceland), VEA (Belgium), FRCT (Portugal), and MINECO (Spain).

About HEATSTORE

High Temperature Underground Thermal Energy Storage

The heating and cooling sector is vitally important for the transition to a low-carbon and sustainable energy system. Heating and cooling is responsible for half of all consumed final energy in Europe. The vast majority – 85% - of the demand is fulfilled by fossil fuels, most notably natural gas. Low carbon heat sources (e.g. geothermal, biomass, solar and waste-heat) need to be deployed and heat storage plays a pivotal role in this development. Storage provides the flexibility to manage the variations in supply and demand of heat at different scales, but especially the seasonal dips and peaks in heat demand. Underground Thermal Energy Storage (UTES) technologies need to be further developed and need to become an integral component in the future energy system infrastructure to meet variations in both the availability and demand of energy.

The main objectives of the HEATSTORE project are to lower the cost, reduce risks, improve the performance of high temperature (~25°C to ~90°C) underground thermal energy storage (HT-UTES) technologies and to optimize heat network demand side management (DSM). This is primarily achieved by 6 new demonstration pilots and 8 case studies of existing systems with distinct configurations of heat sources, heat storage and heat utilization. This will advance the commercial viability of HT-UTES technologies and, through an optimized balance between supply, transport, storage and demand, enable that geothermal energy production can reach its maximum deployment potential in the European energy transition.

Furthermore, HEATSTORE also learns from existing UTES facilities and geothermal pilot sites from which the design, operating and monitoring information will be made available to the project by consortium partners.

HEATSTORE is one of nine projects under the GEOTHERMICA – ERA NET Cofund and has the objective of accelerating the uptake of geothermal energy by 1) advancing and integrating different types of underground thermal energy storage (UTES) in the energy system, 2) providing a means to maximize geothermal heat production and optimize the business case of geothermal heat production doublets, 3) addressing technical, economic, environmental, regulatory and policy aspects that are necessary to support efficient and cost-effective deployment of UTES technologies in Europe. The three-year project will stimulate a fast-track market uptake in Europe, promoting development from demonstration phase to commercial deployment within 2 to 5 years, and provide an outlook for utilization potential towards 2030 and 2050.

The 23 contributing partners from 9 countries in HEATSTORE have complementary expertise and roles. The consortium is composed of a mix of scientific research institutes and private companies. The industrial participation is considered a very strong and relevant advantage which is instrumental for success. The combination of leading European research institutes together with small, medium and large industrial enterprises, will ensure that the tested technologies can be brought to market and valorised by the relevant stakeholders.

Table of Content

1 Introduction

In this report we aim at sharing the results of the activities carried out during and after completion of the drilling operations at the two exploration wells GEo-01 and GEo-02. The wells are in the western part of the Geneva Canton and were drilled as an exploration wells to characterize the geothermal conditions in the Upper Mesozoic carbonates and assess their geothermal potential for applications as hydrothermal resources or storage

GEo-01 well is 744 m deep and drilled into the Cenozoic Units down to 407 MD (Measured Depth) to then enter the Mesozoic carbonates of the Lower Cretaceous unit down to 648 m MD and eventually penetrated the Upper Jurassic carbonates until bottom hole. Artesian fluid flow condition characterizes this well, with a flow rate of 55l/s, 32.4℃ wellhead temperature and 8bars wellhead pressure, representing a very encouraging geothermal resource suitable for heat production and direct uses. Geothermal fluids rise towards the surface along a strike-slip fault structure cutting through the Lower Cretaceous and Upper Jurassic carbonates, being the former responsible of more than 70% of the total mass discharged (Guglielmetti et al. 2020). The natural recharge of the system here is from the Jura Mountain chains and circulation at depth is related to the hydraulic gradient. The faults encountered in the Lower Cretaceous are most likely open faults, laterally confining and vertically promoting localized fluid circulation.

GEo-02 well is 1456 m deep and drilled the same units as GEo-01 reaching the top of the Lower Cretaceous at 769.9m MD. Artesian fluid flow condition characterizes this well, with low flow rate of 0.3-0.6l/s, 18˚C even if the measured bottomhole temperature observed at the end of the drilling operations was about 55˚C and about 12 bars stabilized wellhead pressure and 8bars. As per GEo-01 the natural recharge of the system is expected to be dominated by meteoric waters infiltrating in the Jura Mountain chains and circulation at depth is related to the hydraulic gradient. The fractures encountered in the Lower Cretaceous and Upper Jurassic are most likely mineralized and tight, preventing large fluid flow in this region.

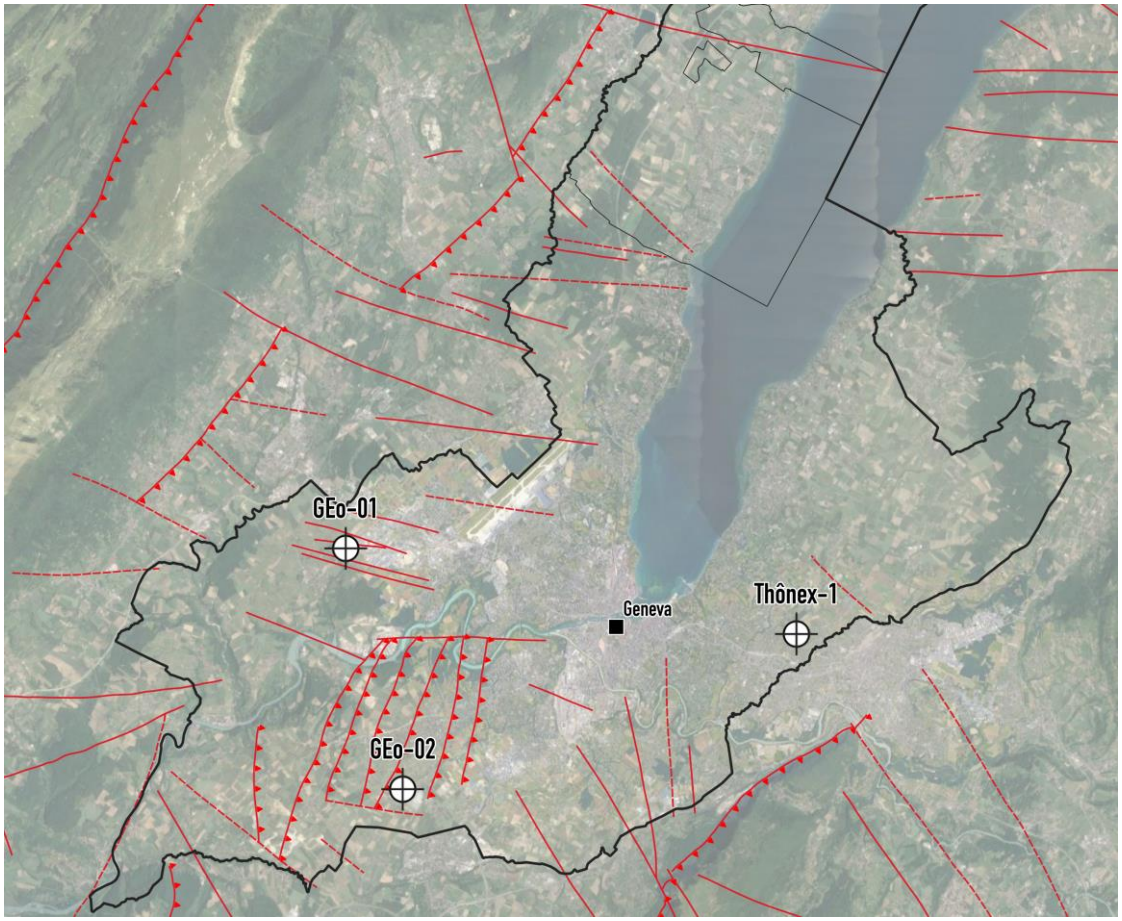

Figure 1. Location of the GEo-01 and GEo-2 wells (modified from Clerc & Moscariello, 2020).

2 Hydraulic testing at GEo-01 and GEo-02

The content of the following chapter presents the results of the short-term hydraulic tests carried out after the well completion and which outcomes allowed calibrating the hydraulic properties of the Mesozoic carbonates at GEo-01. Long-term production tests started in early 2021 and will are still ongoing at present.
From a hydrogeological point of view, the objectives of GE0-01 were to:

- Recognize the hydrogeology of the Cretaceous and Upper Jurassic units in the Geneva basin
- Clarify and/or confirm the hypotheses concerning the hydrogeology of these units, and the local hydrogeological concept, including in particular
  - Reservoir pressure,
  - Flow / productivity,
  - Type of porosity, permeability, degree of fracturing and karstification (and recrystallisation and infilling of these systems),
  - Location and vertical compartmentalization of reservoir levels,
  - Physico-chemical properties of the fluids,
- to allow a better understanding of the hydrodynamics of the Geneva basin, in parallel with other studies in progress or to come:
  - Relation with the recharge, and the Jura massif, including possible compartmentalization between the different sub-basins
  - Sustainability of the resource in case of exploitation,
- The hydrogeological monitoring of the GE0-01 borehole aimed to
  - To collect information related to the hydrogeological reconnaissance of the formations crossed, by placing them in the local context,
  - To be able to set up an adapted reaction in case of events during the operations.

2.1 Groundwater flow observations while drilling

Drilling was performed using mud in the upper 407.5 m where the Cenozoic Molasse sediments were drilled, which did not reveal any evidence of occurrence, loss or other fluid flow evidence of interest. However, During drilling in the Cretaceous and Upper Jurassic formations, various increases in flow were already observed at the surface thanks to their artesian character (Figure 2and Table 1).

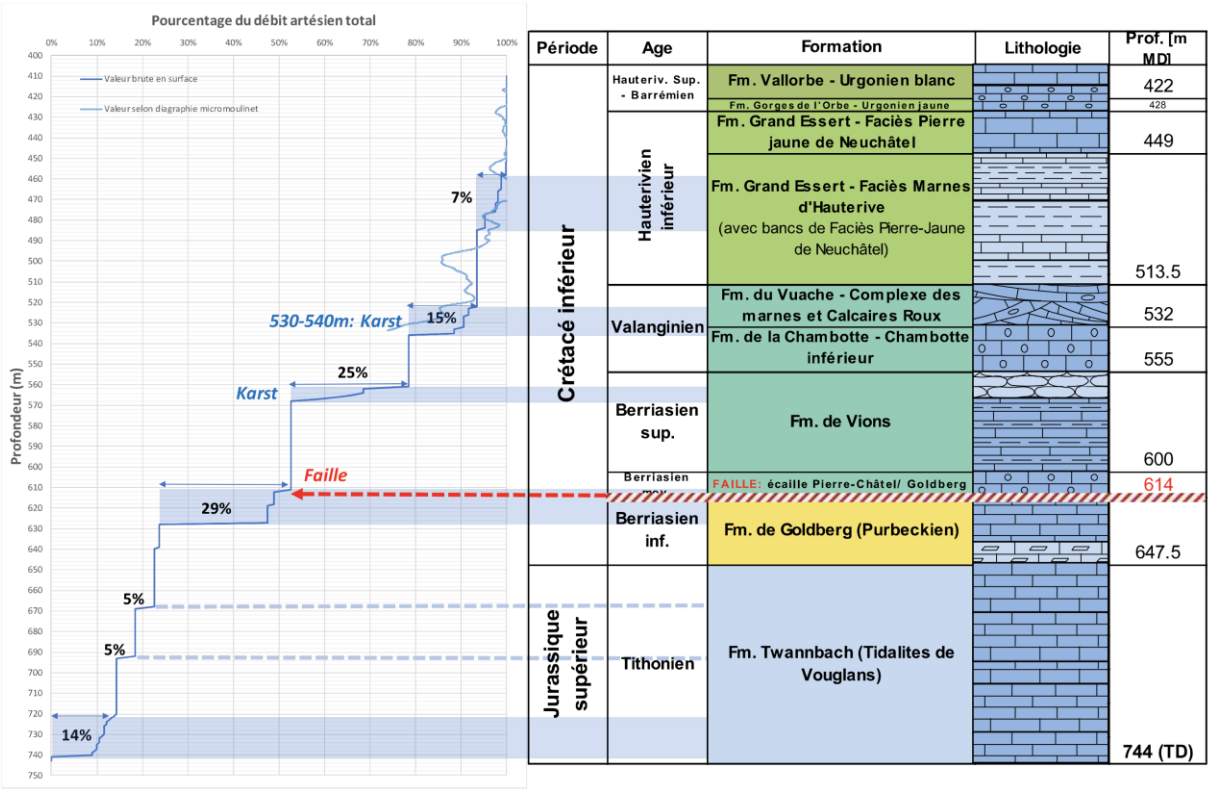

Figure 2. Localisation of water flow level at GEo-01 well (source: SIG).

Table 1. Summary of the water flow levels and reservoir pressure conditions at GEo-01 well (source: SIG).

Water Flow Level	Top	Bottom	Flow rate (m^3/h)	Flow %	Geologic Unit	Type of Permeability	Reservoir Pressure (bar)	Time for pressure to stabilise (seconds)
1	455	486	14	7	Lower Cretaceous	Fractures	9.38	543
2	522	537	30	15	Lower Cretaceous	Karst	9.22	520
3	561	569	50	25	Lower Cretaceous	Karst	10.24	360
4	611	628	58	29	Lower Cretaceous	Fractures	11.75	205
5	662	668	10	5	Upper Jurassic	Fractures	11.45	235
6	692		10	5	Upper Jurassic	Fractures		
7	720	740	28	14	Upper Jurassic	Fractures		

From the first water inflow, the wellhead pressure was around 10 bar, which corresponds to an average hydrostatic level of about 515 a.s.l. (with variations of +/- 20m). This level corresponds approximately to the altitudes of the main springs at the foot of the Jura. Increase in wellhead pressure was observed as new productive fractures were encountered indicating that:

- The upflow is achieved more and more rapidly with increasing arterial flow,
- The higher the artesian pressure, the faster the upflow.

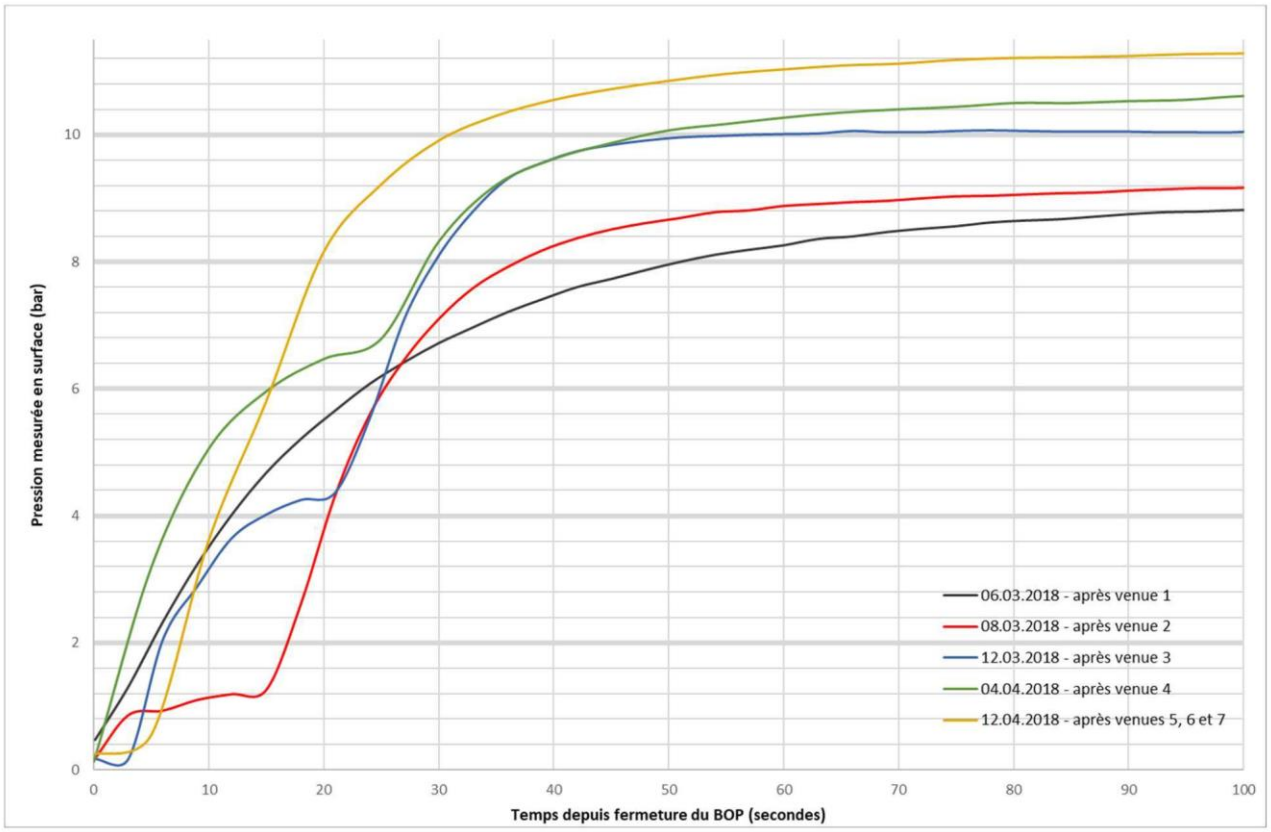

Figure 3. Observed wellhead pressure during drilling (source: SIG).

During the GE0-01 operations, pressure rises could be measured daily during the drilling of the reservoir section and thus allow a fractional hydraulic evaluation of the Lower Cretaceous and Upper Jurassic aquifers. However, due to the presence of the drilling equipment and infrastructure, and the pressure measurement at the BOP, the measured pressure signal was unstable and impacted by pressure losses. A fine analysis of the pressure increase allowing a precise characterization of the reservoir around the well is

therefore not relevant and only an interpretation of the permeability of the medium seems appropriate. Given the high pressure drops, the well and skin storage values are not representative of the well and the near reservoir and are therefore only used as a calibration element. The initial reservoir pressures vary over time between 9.2 and 11.7 bar so the late phase of the pressure rise will not be characterized as it would be too biased by these regional variations in reservoir pressure. In order to best interpret the available pressure rises, and therefore the intrinsic permeability of the GE0-01 geothermal reservoir, three types of analysis have been performed proposed:

- Analysis 1: Simple analysis of the medium to approximate the overall permeability of the section studied.
- Analysis 2: In addition to analysis 1, this analysis will use a partial penetration well model representing the punctual inflow of water in the section studied, which will allow the evaluation of the anisotropy of the medium and the estimation of the length of the perforated zone (which can be associated with the thickness of the fractured zone)
- Analysis 3: Multi-layer analysis to define the permeability of each section, taking into account the analyses performed on the previous sections. The sections without water inflow will be considered as quasi-permeable.

The results are resumed in Table 2-Table 4.

Table 2. Parameters used for Analysis 1 (source: SIG).

Analysis 1				
Investigated interval (m b.g.l.)	Wellbore storage (m^3/bar)	Skin	Average permeability (mD)	Permeability sensitivity (mD)
411-507.4	0.008	68	400	300-500
411-537.4	0.19	71	1048	700-1500
411-477.4	0.26	107	2086	1500-2500
411-637.4	0.105	73	2257	1750-2750
411-744	0.089	104	1900	1400-2400

Table 3. Parameters used for Analysis 2 (source: SIG).

Analysis 2						
Investigated interval (m b.g.l.)	Wellbore storage (m^3/bar)	Skin	Length of the drilled section	Average permeability (mD)	Permeability sensitivity (mD)	Anysotropy (k_z/k_r)
411-507.4	0.008	15	15	420	300-600	0.014
411-537.4	0.18	20	20	1470	1200-1700	0.0033
411-477.4	0.26	47	47	1980	1700-2300	0.016
411-637.4	0.1	54	54	2850	1250-3350	0.033
411-744	0.08	166	166	2050	1500-2500	0.12

Table 4. Parameters used for Analysis 3 (source: SIG).

Analysis 3							
Type of formation	Top (m)	Base (m)	Wellbore storage (m^3/bar)	Skin	Porosity	Average permeability (mD)	Permeability sensitivity (mD)
Acquiclude 1	411	455	0.1	0	1	1	-
Flow level1	455	486		80	10	1361	900-2200
Acquiclude 2	486	522		0	1	1	-
Flow level 2	522	537		91	10	7163	5000-1000
Acquiclude 3	537	561		0	1	1	-
Flow lelve 3	561	569		75	10	13800	9000-25000
Acquiclude 4	569	611		0	1	1	-
Flow level 4	611	628		80	10	16000	9800-18200
Acquiclude 5	628	668		0	1	1	-
Flow levels 5-7	668	740		80	10	100	50-150

2.2 Hydraulic tests during drilling

The artesian conditions made it easy to carry out hydraulic tests as drilling operations advanced. These tests made it possible to accurately monitor the evolution of the well flow as it deepened.
These tests were carried out in two formats:

- Pressure and artesian flow measurements before and/or after the drilling days
- Step drawdown tests with increasing artesian flow until stabilization carried out after each observation of water flow in excess of 10m^3/h, after each major lithological change, or after a drastic change in the drilling parameters (e.g. significant increase in rate of penetration)

These tests were carried out by evacuating the water:

- Through the Choke Line (whose technical characteristics implied significant pressure losses) up to the up to a flow rate of 45 m^3/h.
- Then by flowing through the Flow Line and then back through the cellar pump from 45 m^3/h.

Pumping tests were also carried out at the end of the Cretaceous drilling at 637m depth.
Table 5 shows the results of all these measurements and tests.

Table 5. Synthesis of the results of hydraulic testing during drilling (source: SIG).

Depth 455m (MD)				
Step	**Flow rate (m^3/h)**	**Pressure (bar)**	**Duration (h)**	**Productivity index (m^3/h/bar)**
0	0	9.03		
1	0.2	0.1	0.25	0.025
Depth 472m (MD)				
0	0	8.03		
1	2	4.92	0.5	0.643
2	4	0.27	0.5	0.515

Depth 487m (MD)				
0	0	9.43		
1	3	8.07	0.5	2.206
2	6	5.91	0.5	1.705
3	9	1.41	0.5	1.122
4	11.4	0.13	0.5	1.226
Depth 502m (MD)				
0	0	9.2		
1	11	0.13	0.25	1.213
Depth 537m (MD) - Test 1				
0	0	9.34		
1	19	0.13	0.25	2.063
Depth 537m (MD) - Test 2				
0	0	9.32		
1	4	9.09	0.75	17.391
2	8	8.55	0.75	10.39
3	15	6.98	0.75	6.41
4	26	1.9	0.75	3.504
5	27.7	0.1	0.75	3.004
Depth 552m (MD)				
0	0	9.32		
1	41	0.13	0.25	4.461
Depth 562m (MD)				
0	0	10.31		
1	92	0.13	0.25	9.037
Depth 594m (MD)				
0	0	11		
1	16.7	10.54	0.75	36.304
2	31.8	9.51	0.75	21.342
3	48.5	7.86	0.75	15.446
4	56.6	6.79	0.75	13.444
5	92	0.13	0.75	8.464
Depth 627m (MD)				
0	0	10.86		
1	102	0.13	0.25	9.506
Depth 637m (MD) - Test 1				
1	115	0.13	0.75	10.658
2	48.8	7.33	0.75	16.379
3	38.7	9.03	0.75	20.476
4	0	10.92	0.75	
Depth 637m (MD) - Test 2				

0	0	10.65		
1	132	0.13	0.25	12.548
Depth 637m (MD) - Test 3				
0	0	8.79		
1	5.8	9.73	0.5	96.667
2	9.9	9.66	0.5	76.154
3	15	9.55	0.5	62.5
4	23	9.32	0.5	48.936
5	39.5	8.65	0.5	34.649
6	59.5	7.5	0.5	25.983
Depth 637m (MD) - Test 4				
0		9.78		
1	131	-0.182	0.75	13.149
2	135	-0.478	0.75	13.161
3	140	-1.49	0.75	12.422
4	145	-2.197	0.75	12.106
5	148	-2.781	0.75	
Depth 637m (MD) - Test 5				
0		9.78		
1	127	-0.11	0.75	12.841
2	145	-2.088	0.75	12.218
Depth 637m (MD) - Test 6				
0	0	10.62		
1	15.2	10.36	0.75	58.462
2	30.5	9.86	0.75	40.132
3	45.7	9.1	0.75	30.066
4	62	8.1	0.75	24.603
5	140	0.13	0.75	13.346
Depth 690m (MD)				
0	0	10		
1	165	0.13	0.25	16.717
Depth 712m (MD)				
0	0	11.14		
1	175	0.13	0.25	15.895
Depth 744m (MD) - Test 1				
0	0	11.66		
1	188	0.13	0.25	16.305
Depth 744m (MD) - Test 2				
0	0	11.66		
1	205	0.13	0.25	17.78

The graph below (Figure 5.21) shows the results of these different tests in the form of an overlay of characteristic curves. It should be noted that the y-axis shows the measured pressure / observed dynamic level, not the obtained drawdown. The differences in natural pressure, measured between 9.32 and 11.66 bar, are therefore not erased.
Furthermore, the results presented are raw surface results, not corrected for the various induced pressure losses (presence of the tool, presence of the drill string, choke line, weight of the water column, etc.). The long-term production tests will make it possible to refine all the results obtained during drilling and during the short-term tests.

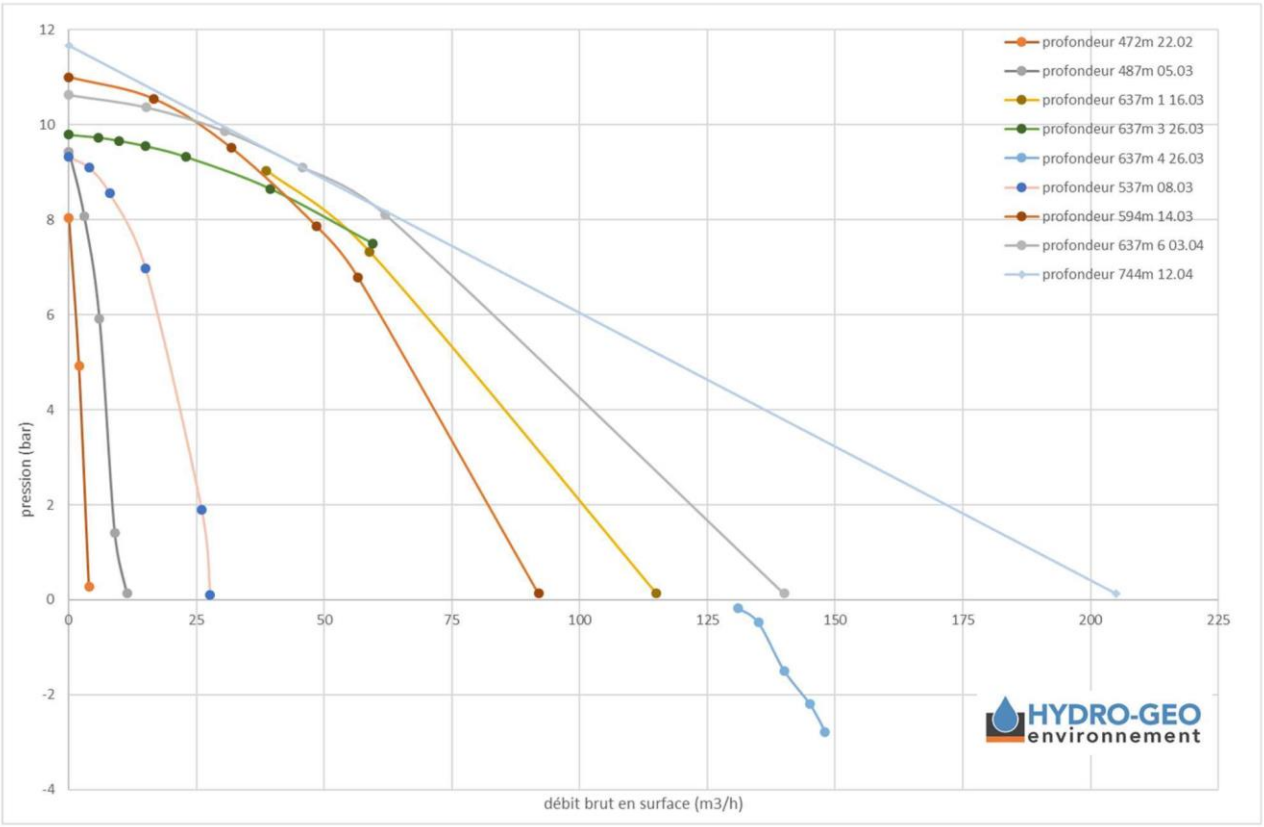

Figure 4. Results of hydraulic testing during drilling (source: SIG).

The plot in Figure 4 Figure 7shows the evolution of the productivity of the GEo-01 well as it drilling operations advanced. It also shows that for the first tests carried out, the 'critical' flow rate appears very quickly because of the pressure losses induced by the drill string and other technical equipment (including the Choke Line) and induced by the critical circulation speeds within the producing fractures.
Thus, the gross productivity index reaches:

- at the end of drilling in the Cretaceous, about 1.20 m^3/h/m of drawdown,
- at the end of drilling (Cretaceous + Upper Jurassic), about 1.82 m^3/h/m of drawdown

2.3 Short-term production tests

At the end of the drilling operation on the lower Cretaceous formations (at 637.4m), hydraulic pumping test tests were carried out with an average flow of 148 m^3/h. This average flow rate of 148 m^3/h was only 15-25 m^3/h higher than the natural artesian flow rate.
The graph in Figure 5 shows the evolution of pumped flow and drawdown level during this short 48 hour test. This plot shows that the water level in GEo-01 does not show any stabilisation of the drawdown level: after a drawdown of 23.4m at the start of the pump, the level evolves slowly to reach a rise of 1.7m. This rise :

- Is due to the increase of the reservoir load at this period, visible on the Mathieu well,

- It has a slight influence on the pump's flow rate, by regulating the flow rate/HMT couple: when the level rises naturally, the pump operates more easily and its flow rate increases slightly (from 147 to 149 m3/h)
- Does not allow the interpretation of the test from a hydrodynamic point of view, nor the calculation of transmissivity/permeability parameters.

During this test, the in situ physico-chemical parameters evolved as follows:

- pH and conductivity remained very stable at 7.4 and 360 us/cm respectively.
- Turbidity evolved between 5 and 25 NTU.
- The dissolved oxygen concentration evolved between 0.1 and 0.3 mg/l.
- Redox stabilised very quickly in the range -340/-350 mV.

The extraction of a volume of 7,100 m³ (of which 1,300 m³ is more than the natural artesian flow) does not therefore generate any notable impact on the Cretaceous reservoir, which therefore appears to be very important.

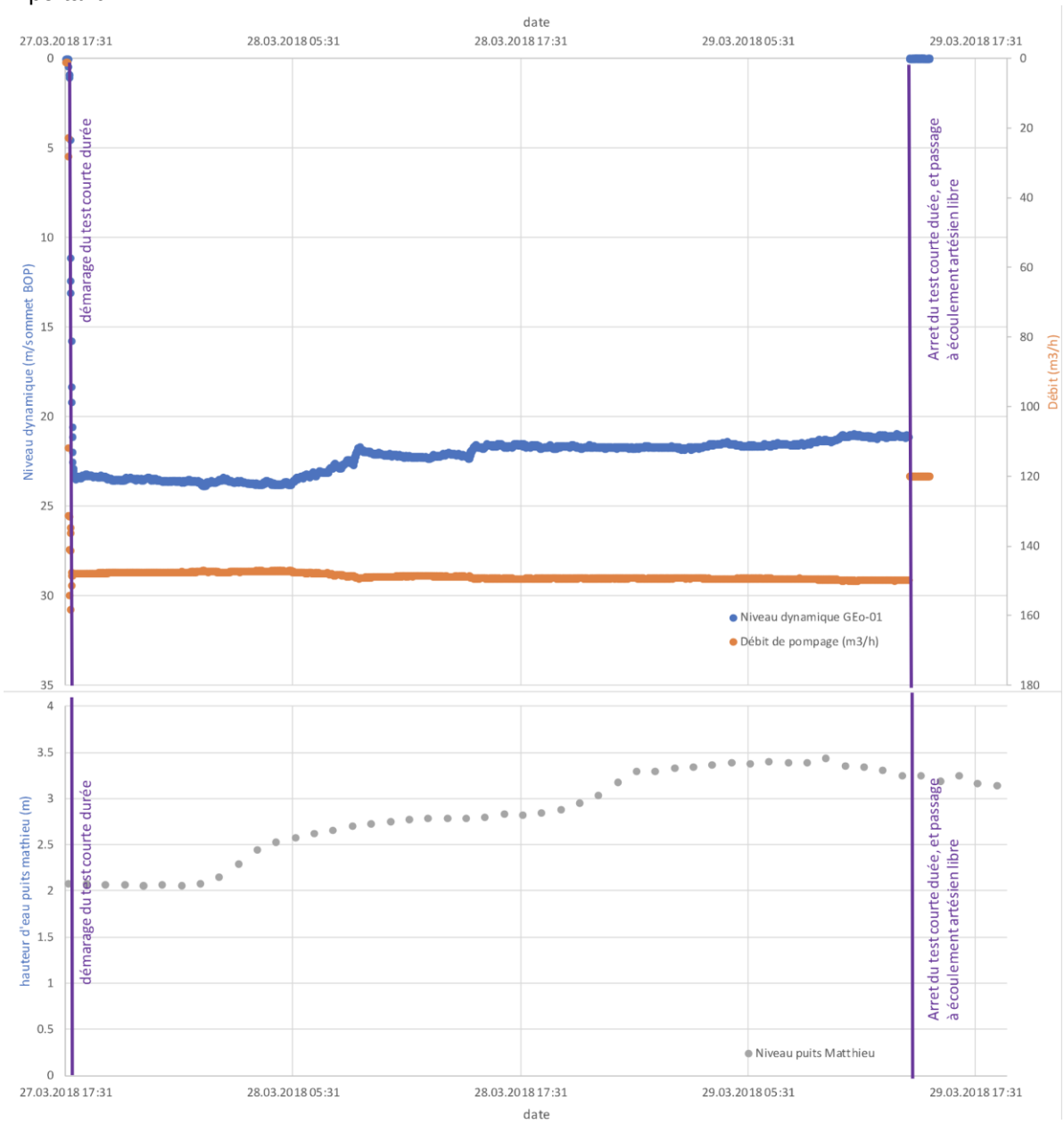

Figure 5. Results of the short-term production tests in the Lower Cretaceous section (source: SIG).

3 Hydraulic fracturing stress Tests at GEo-02

As part of the geological and hydrological characterization of the fractured carbonate reservoir targeted by the Geo-02 well, Services Industriels de Geneve (SIG) awarded Solexperts AG to carry out hydraulic fracturing stress measurements in the vertical borehole GEo-2 of 1455 m depth, besides comprehensive hydraulic tests. Main objective of the hydraulic fracturing tests was to determine the magnitude and the orientation of the in-situ stress. In summary, a total of 8 hydraulic-fracturing tests was conducted during 15.-20.07.2020. For fracture orientation determination, BHTV-logging was conducted prior and after hydraulic fracturing. The present chapter resumes the results of the test which are described in detail in the final report provided by Solxeperts available in the Annexes.
The borehole penetrates the following geologic units:

- Sedimentary rocks of the Quaternary (0-38 m, average density 2.4 g/cm3),
- Molasse (38-630 m, 2.55 g/cm3),
- Siderolithic (630-769.9 m, 2.5 g/cm3)
- Lower Cretaceous (769.9- 996 m, 2.66 g/cm3)
- Upper Jurassic (996-1455 m, 2.66 g/cm3).

Thus, the vertical stress Sv due to the weight of the overburden rock can be estimated to 37 MPa at the bottom of the borehole at 1455 m.
Seven test sections between 1335 m and 1424 m depth were selected for the tests, and one test section within the Cretaceous rocks at 883 m was selected although the borehole diameter of about 7-3⁄4 inch only allows packer pressurization up to 20 MPa.

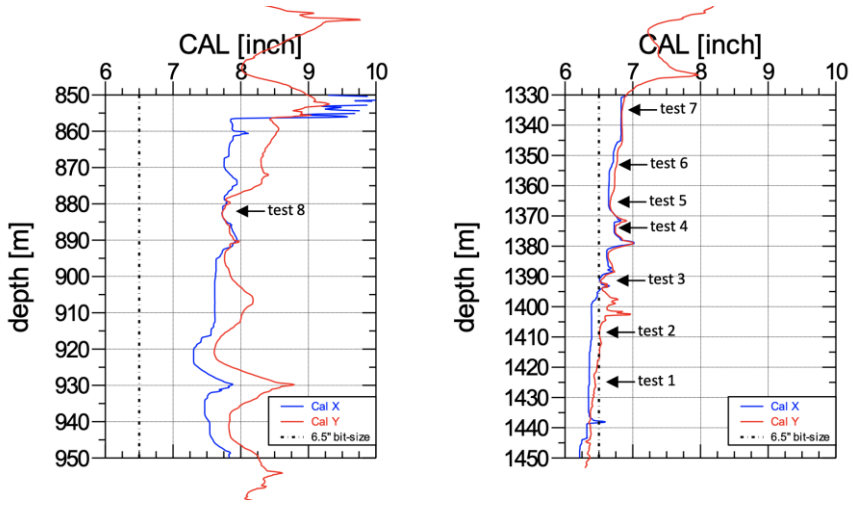

Figure 6. Caliper-log borehole GEo-2 (source: Solexpert, 2020).

The derived characteristic hydrofrac pressure data (breakdown pressure P_c at fracture initiation, fracture re-opening pressure P_r, shut-in pressure P_{si}, and the resulting in-situ tensile strength $T = P_c - P_r$) are shown graphically in Figure 7.
Of the 8 tests, the 5 tests at 1335.0 m, 1366.0 m, 1374.0 m, 1409.0 and 1424.0 m are characterized by (weak) fracture initiation events with low breakdown pressure values ranging from 21.0 MPa to 24.9 MPa. In the remaining 3 test sections at 883.0 m, 1353.0 m and 1391.0 m preexisting fractures without distinct pressure peaks were stimulated. The refrac-pressure values vary between 12.8 MPa at 883.0 m and 23.5-24.0 MPa at 1353.0 m, the corresponding in-situ hydraulic tensile strength T between 2.8-3.1 MPa and 4.6-4.9 MPa with a mean value of T = 3.8 ± 0.7 MPa. The tests yield rather distinct and reliable shut-in pressure values which scatter significantly between 1335.0 m and 1424.0 m depth between 17.9 MPa to 27.7 MPa, besides the value of 13.2 MPa at 883.0 m depth. As shown in Figure 9, the characteristic hydrofrac pressure values are considerably lower than the calculated vertical stress Sv due to the weight of the overburden rock mass. The low shut-in pressure indicates the initiation or stimulation of non-horizontal fractures.

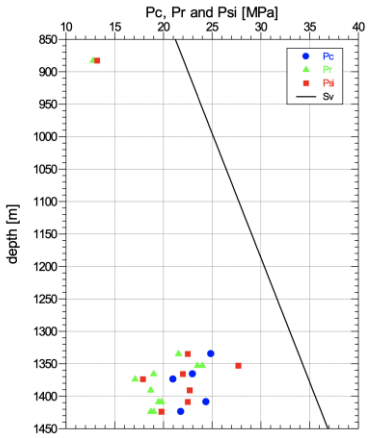

Figure 7. Breakdown - pressure P_c, refrac-pressure P_r and shut-in pressure P_{si} in borehole GEo-2 in relation to the vertical stress S_v

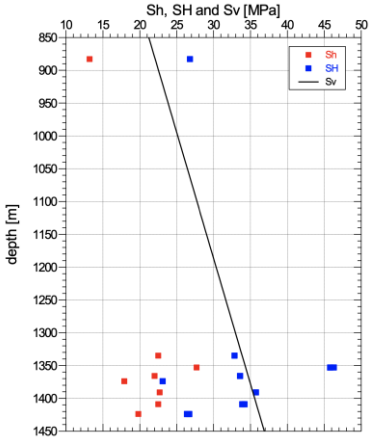

Figure 8. Principal stresses for borehole GEo-2.

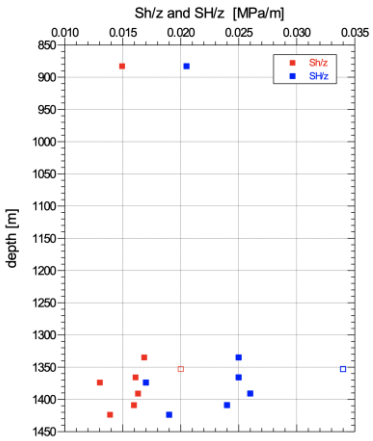

Figure 9. Horizontal stress gradients S_h/z and S_H/z for borehole GEo-2.

4 Hydro-chemical Monitoring at GEo-01 and GEo-02

4.1 GEo-01 hydro-chemical features

In the framework of HEATSTORE a series of groundwater sampling surveys were carried out at the GEo-01 with the initial goal to characterize and better constrain the fluid circulation paths, time and water-rock interaction of geothermal waters across the entire Geneva Basin and eventually monitor the production tests still ongoing at present at GEo-01. Data were collected by University and Geneva and Hydrogeo Environnement under a contract with SIG. Analysis were carried out at the laboratories of Hydroistop GmbH.

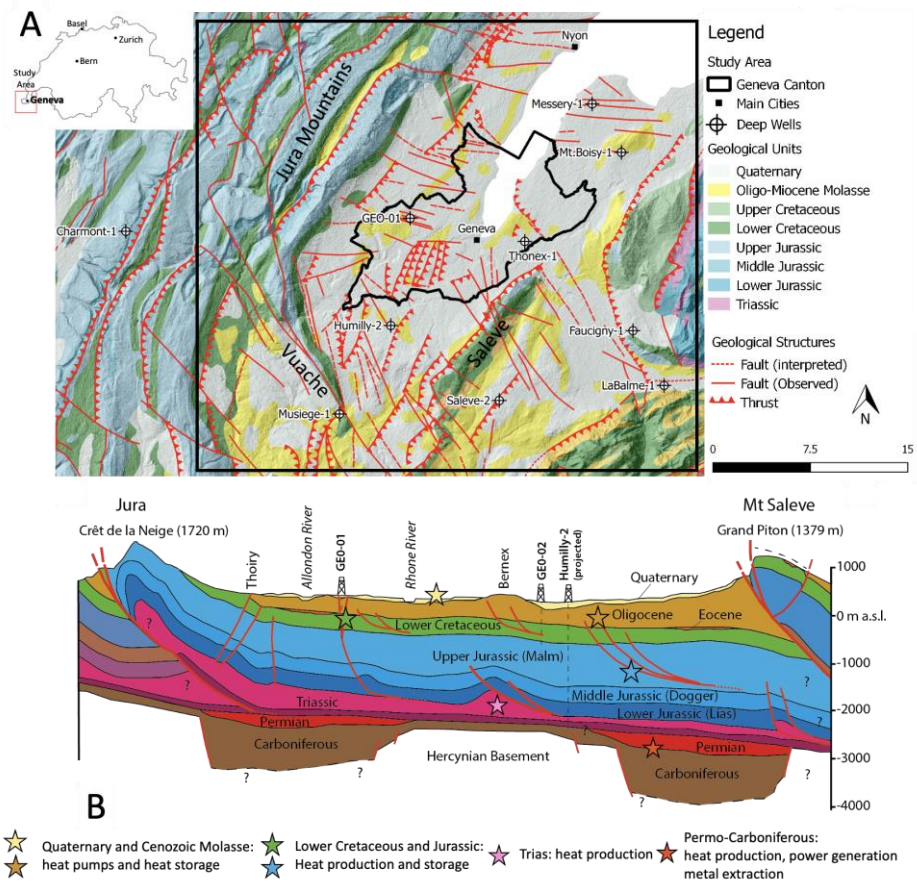

Figure 10. A) Geological map over the Geneva Basin with indication of the main deep wells and sampled features (modified. from Brentini, 2018); B) Cross section cutting though the GB (modified from Clerc & Moscariello et al., 2020)

4.1.1 Major Ions

Deep fluids circulating in carbonate aquifers such as those in the Cretaceous and Jurassic units in the study area, usually show geochemical facies dominated by Calcium (Ca) and Bicarbonate (HCO_3). However, fluids having deep and long paths (several kilometres), as well as a long residence time (thousands of years), show more complex geochemical composition due to the longer time and larger depth, hence temperature, which allow more complex water-rock chemical reactions. Additionally, such deep fluids flow towards the surface though fault corridors, where secondary minerals dominate the water-rock interactions during the last stages of the circulation. In sedimentary basins, where waters can reach several km in depth and temperature even above 100˚C, the main geochemical signature is dominated by Sodium (Na) and Chloride (Cl).

Both facies are observed in the Geneva area. The three springs show a clear Ca-HCO_3 composition even if the Jules Cesar Spring, shows a slightly higher temperature, a noticeable enrichment in Na-Mg-Cl-SO_4-SiO_2, a higher salinity, compared to the other two springs. GEo-01 well a predominant Na>Ca- HCO_3 and Thonex-01 well a predominant Na-Cl signature (Figure 11).

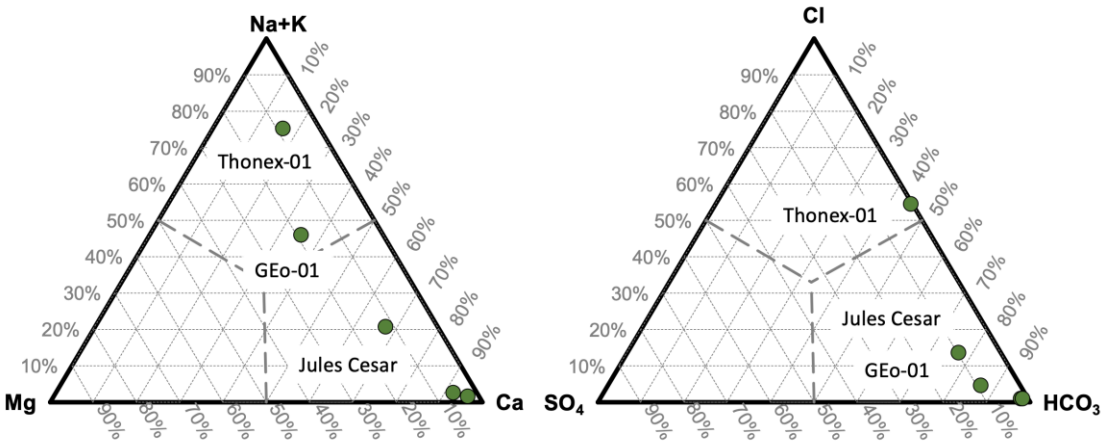

Figure 11. Ternary plots of the analysed samples.

4.1.2 Trace Elements

Trace elements have been analysed with particular focus on enhancing the differences between the springs and the wells.
The Thonex-01 wells show an enrichment in Br^-, NH_4^+ and Iron, whereas GEo-01 well shows concentrations similar to those from springs except for the Bromide which is higher.
Ammonia (NH_4^+) shows higher values in the two wells most probably associated to the presence of organic matter and hydrocarbons.
Cl/Br ratio observations were also carried out in this study, as it is an effective method to decipher the origin of the salinity. In fact values above 655 indicate halite dissolution, close to 655 is the value typical of seawaters, below 655 indicate that brines contribute to the Chloride content (Alcalá & Custodio, 2008; Sonney & Vuataz, 2010a). In this case, the analyzed waters show values between 4 (GEo-01) well and 600 (Jules Cesar Spring), suggesting that the circulating waters do not flow through any salt-rich formation, usually located in the Triassic Units, hence the circulation is limited to the Upper Mesozoic limestones.

4.2 Geochemical interpretations

4.2.1 Chemical equilibria

Fluid-mineral equilibria were computed with PHREEQC (Parkhurst & Appelo, 1999) code choosing the most representative samples in terms of temperature and mineralization
Saturation Indexes for the Thonex-01 well were computed for the wellhead temperature of 14.3˚C and for increasing temperature up to the bottomhole temperature of 88˚C recorded after drilling operations (Jenny et al., 1995). The results are reported in Table 6.
.
All the spring and the GEo-01 well are in equilibrium with Calcite and undersaturated in Dolomite and evaporitic lithologies. With respect to Silica phases, all the springs are close to saturation with respect to Quartz. Thonex-01 well is slightly oversaturated in Calcite, Aragonite and Dolomite at both wellhead and bottomhole temperatures. This well is strongly undersaturated in gypsum and Anhydrite and at wellhead temperature it is in equilibrium with Chalcedony.

Table 6. Saturation Indexes for selected minerals.

	Saturation Index					
	Puits Matthieu	**Doua Spring**	**Jules Cesar Spring**	**GEo-01 Well**	**Thonex-01 Well (wellhead)**	**Thonex-01 Well (Reservoir at 90˚C)**
Temperature	8.6	9.5	12.1	32.4	14.6	88.0
pH	7.5	7.3	7.3	7.5	7.7	7.5
Calcite	-0.054	-0.073	-0.011	-0.072	0.346	0.944
Aragonite	-0.209	-0.229	-0.164	-0.215	0.191	0.836
Dolomite	-1.258	-1.695	-0.627	-0.075	0.514	1.931
Gypsum	-3.041	-3.025	-1.801	-2.611	-4.150	-4.162
Anhydrite	-3.534	-3.509	-2.252	-2.910	-4.626	-3.850
Amorphous Silica	-2.111	-1.818	-1.311	-1.255	-0.803	-1.366
Chalcedony	-1.213	-0.923	-0.426	-0.417	0.089	-0.702
Quartz	-0.730	-0.443	0.044	0.010	0.568	-0.435

4.3 Reservoir Temperature

The alkaline geothermometers of Na-K and Na-K-Ca with Mg correction were employed and compared to the other equations as it is demonstrated that the Na-K geothermometer, developed by Fournier, (1979) and (Giggenbach, 1988) highly overestimates the temperature for low enthalpy fluids (Sonney & Vuataz, 2010). At temperatures below 120˚C the sodium and potassium concentration are controlled by minerals such as clays and not only by the feldspar ion-exchange reactions which occur at higher temperatures (Nicholson, 1993).
To overcome this the Na-K-Ca geothermometer was developed by (Fournier & Truesdell, 1973) and later corrected by (Paces, 1975) to permit this equation to be reliably applied. The results shown in Table 7 show a good agreement between calculated and measured reservoir temperature for the GEo-01 and Thonex-01 well.

Table 7. Reservoir temperature (˚C) estimated by Na-K-Ca and measured (n.a. = not applicable).

Sample Name	**Na-K-Ca**	**Measured Temperature**
Puits Matthieu	n.a.	8.6
Source de la Doua	n.a.	9.5
Source Jules Cesar	21	12.1
GEo-01 Well (wellhead)	36	32.4
GEo-01 Well (bottomhole)		34.0
Thonex-01 Well (wellhead)	84	14.6
Thonex-01 Well (bottomhole)		88

4.4 Origin of the fluid

The origin of thermal waters and elevation of the recharge zone can be estimated by means of the stable isotopes of hydrogen and oxygen. The results of the analysed samples for this study are compared to the world meteoric water composition (WMWC) and to the Swiss meteoric water composition (SMWC) by Kullin & Schmassmann, (1991), which slightly differentiates from the WMWC. The samples show $\delta^{2}H$ values between -82 δ‰ (Thonex-01 well) and -68.6 δ‰ (Jules Cesar Spring) and $\delta^{18}O$ values between -11.33 δ‰ (GEo-01 well) and-9.54 δ‰ (Jules Cesar Spring). All samples plot along meteoric lines, indicating a clear meteoric origin (Figure 12).

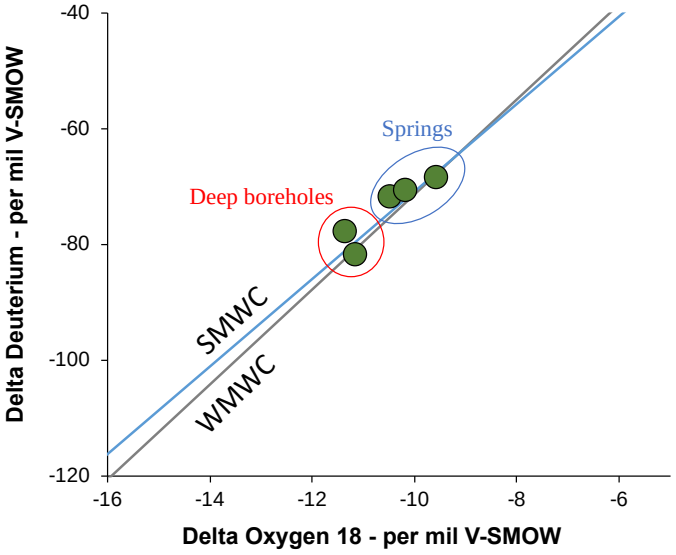

Figure 12. Stable isotopes of Oxygen and Hydrogen showing the meteoric origin of the sampled waters.

To estimate the elevation of the recharge zone with the stable isotopes, hydrogen and oxygen can be used. Several equations have been developed for different regions based on the main assumption that the concentration in such isotopes remains constant with time. However, for very long residence times (>10'000 years), the results can be biased due to the infiltration in climatic conditions different from more recent times. Additionally, the $\delta^{18}O$ isotopic composition can be affected by isotopic fractioning. Therefore, $\delta^{2}H$ isotopes are considered as more reliable for elevation estimation. The equations used for this study are those for the Jura region (Blavoux, et al., 1979; Kullin & Schmassmann, 1991), Swiss Plateau (Blavoux, et al., 1979; Kullin & Schmassmann, 1991), Swiss Plateau (Kullin & Schmassmann, 1991), Swiss Plateau & Northern Alps (Vuataz, 1982) and Leman Prealps (Blavoux, 1978). Table 8 shows the results indicating an average recharge zone between 800 and 1400m, which is relatively coherent with the average elevation of the Jura Mountains. However, it should be noted that the results for the Geo-01 and Thonex-01 well are about 400-500m higher than those for the springs, suggesting that the recharge probably occurred in climatic conditions slightly different than at present (about 2˚C colder than now).

Table 8. Recharge elevation estimation based on of $\delta^{2}H$ and $\delta^{18}O$ isotopes.

	Puits Matthieu	Doua Spring	GEo-01 Well	Thonex-01 Well	Jules Cesar Spring	Authors	Isotope
Central Jura	1125	975	1565	1460	670	Kullin & Schmassmann, 1991	$\delta^{18}O$
	957	878	1323	1561	744		$\delta^{2}H$
French Jura & Swiss Central Jura	1017	850	1506	1389	511	Blavoux et al., 1979	$\delta^{18}O$
	813	727	1213	1473	580		$\delta^{2}H$
Swiss Plateau	625	518	939	864	300	Kullin & Schmassmann, 1991	$\delta^{18}O$
	478	409	801	1011	290		$\delta^{2}H$
Swiss Plateau & Northern Alps	728	618	1051	974	393	Vuataz, 1982	$\delta^{18}O$
	661	601	936	1115	500		$\delta^{2}H$
Leman Prealps (Thonon/Evian)	783	683	1077	1007	480	Blavoux, 1978	$\delta^{18}O$
	680	628	920	1076	540		$\delta^{2}H$

4.5 Residence Time

Groundwater residence time can be approached by means of Tritium, SF_6 and Carbon- 14 analyses. The spring waters have ^3H and SF_6 concentrations between 5.3 and 6.3 TU and between 3.0 and 3.7 fmol/L, respectively (Table 4). The modelling of the mean residence times using 75 % exponential and 25 % pistonflow model, which might reflect the investigated spring systems shows that the springs water consist of mainly young groundwater with residence times between 5 and 15 years (Figure 13).

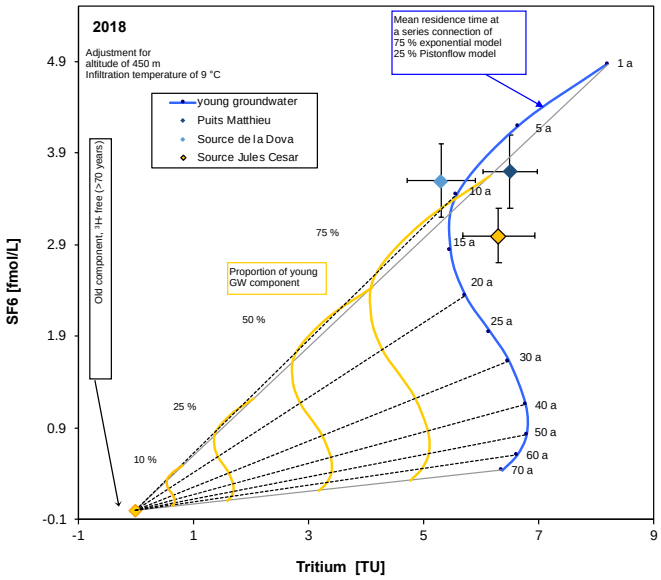

Figure 13. Modelling of mean residence times of spring waters sampled in the Geneva Basin.

Tritium could not be detected in the groundwater sampled in the deep boreholes, indicating that there is no inflow of young water. Previous studies (Muralt 2000 and Vuataz & Giroud, 2010) determined a residence time between 10'000 and 15'000 years for Thonex-01 well using Carbon isotopes ($\delta^{13}C$=-2.3 ‰ PV-PDB and ^{14}C=2.2 pmC). These results are similar with those observed in 2018 for the Thonex well ($\delta^{13}C$ =-4.4pmC and ^{14}C=2.2 pmC). ^{13}C values decreased with respect to 2010 probably due to degassing, lowering pCO_2 during upflow, therefore enabling HCO_3 precipitation, making the $\delta^{13}C$ in the water lighter than in the reservoir rock where literature data report values of -0.2‰ V-PDB. Thermal water sampled in the GEo-01 borehole has a ^{14}C concentration of 18.01 pmC and a $d^{13}C$ isotope ratio of -4.4‰ V-PDB suggesting a shorter residence time than for the Thonex-01 well..

4.6 Discussion

The sampled waters in this study show geochemical composition that reflects circulations within the Upper Mesozoic units which origin can be located between 800 and 1200m the Jura Mountains. The infiltration for the three springs occurred in recent times as confirmed by Tritium data, which also reveal a longer residence time for GEo-01 and Thonex-01 wells. If for the former well the residence is not at the moment fully constrained, previous studies on the Thonex-01 well estimated a residence time of 10'000-15'000 years.
The geochemical composition of the sampled features reveals that three main geochemical facies can be identified:
Puits Mathieu, and Doua springs show a classical Ca-HCO_3 composition dominated by water-rock interactions that occur during rapid circulation in the Mesozoic units as also confirmed by the equilibria with respect to the carbonate mineralogical phases.
Jules Cesar spring shows a dominant Ca-HCO_3 with higher temperature and concentrations in Na-Cl-SO_4-SiO_2 compared to the two other springs. This can be interpreted as partially related to anthropic pollution due road salt contamination but also to the result of mixing processes between two end-members which recharge zone from the Saleve ridge cannot be excluded: a recent (according to Tritium values) and shallow Ca-HCO_3 end-member and a deeper and slightly warmer Na-Cl>SO_4 end-member probably originating by leaching of deeper Mesozoic Units.

At GEo-01 the observed composition in Na>Ca-HCO_3 reflects a circulation within the Jurassic units, recharged in the Jura Mountains before the atmospheric nuclear tests (1953-1964). The waters discharged are in equilibrium with the carbonate mineralogical phases. The reservoir temperature estimated by the Na-K-Ca geothermometer is consistent with the one measured at the wellhead during the sampling campaign thanks to the large artesian flow observed. The discharged waters result from a mixing of relatively different water between different productive fractures in the Lower Cretaceous giving a pure Ca-HCO_3 composition and in the Upper Jurassic which can contribute to the Na, Mg concentrations. The presence of Mg rich end-member can be representative of the Oxfordian dolomite-rich lithologies which were not drilled by the GEo-01 well but that are most probably cut by fault structures that act as a preferential up-flow pathways towards the surface.
At the Thonex-01 well the Na-Cl geochemical imprint is correlated to long circulation both in terms of distance from the recharge zone and residence time. In fact, the waters discharging from the well are recharged by meteoric waters which infiltrated in the Jura Mountains in climatic conditions colder than at present and the residence time has been estimated to be between 10'000 and 15'000 years. During this time the infiltrated waters cover the distance of about 20km from the Jura Mountains to the well and have the time to get into full thermal equilibrium with the reservoir host-rock in the Jurassic formations. The Na-Cl composition results from Ca-Na ion exchange reaction that might occur at the Oxfordian formations which have been drilled in the last 400m of the well. This is also supported by the Magnesium concentration (higher than in the other sampled features, which can result from the water-rock interactions with dolomite-rich lithologies such as those in the Oxfordian.

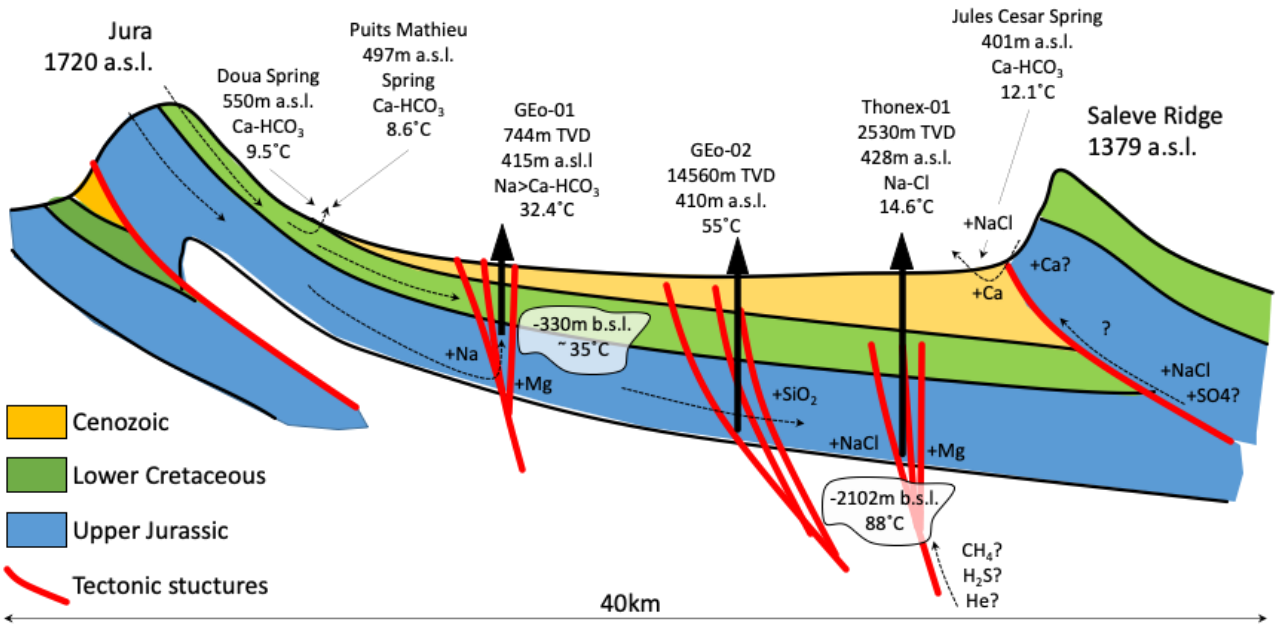

Figure 14. Conceptual model of groundwater circulation in the Geneva Basin (vertical and horizontal scales are not proportional).

In this first step of screening, the results of the geochemical investigation on the liquid phase discharged from springs and two geothermal exploration wells are presented. The study focusses on the understanding the geochemical evolution of groundwater across a NW-SE oriented cross-section passing though the main infiltration zone of meteoric waters in the Jura Mountains towards NW, the Puits Mathieu and Doua springs located at the Jura foothills, the geothermal exploration wells GEo-01 drilled in 2018, and Thonex-01 drilled in 1993 and the Jules Cesar spring located at the SE of the section. All the analysed samples show a meteoric origin, and the main recharge zone is located in the Jura Mountains. Only the Jules Cesar spring shows geochemical composition that can be most probably associated to an infiltration of meteoric waters at the Saleve Ridge and in part to anthropic contamination. The Puits Mathieu and Doua cold spring show the typical Ca-HCO_3 composition due to circulation in Lower Cretaceous, most probably controlled by karstic pathways allowing very rapid circulation as shown on Tritium data. The GEo-01 is 744m deep and discharges thermal waters at 32.4˚C with an artesian flow of 55.6 l/s and a wellhead pressure of 10bars. The geochemical composition of the discharged waters is most probably associated to a mix of pure Ca-HCO_3

groundwater from the Lower Cretaceous with a second endmember representative of water interacting with dolomite-rich lithologies such as those located at the base of the Upper Jurassic. The residence time of the water discharged by the GEo-01 well are not associated to recent and rapid circulations as shown by Tritium data, but Carbon isotopes reveal a residence time of probably some thousands of years. The Thonex-01 has been drilled to reach the Upper Jurassic reservoir at more than 2500m in depth. The bottomhole temperature recorded after drilling was 88˚C and residence times of more that 10'000 years have been estimated confirming previous analyses. The well discharge water at 14.6˚C having a Na-Cl geochemical composition due to the water-rock interactions that occur within the Upper Jurassic lithologies that compose the main reservoir. The Jules Cesar cold spring discharges a complex mix of waters most probably due to mixing processes between a cold, shallow and recent Ca-HCO_3 endmember and a deeper and warmer Na-Cl>SO_4 endmember. The results of this study highlight how deep circulation in the Geneva Basin have a common meteoric origin but complex circulations due to the heterogeneities i.e., in the reservoir rock in terms of mineralogical composition, tectonic setting and lithology. To further constrain the understanding of deep circulations in the Geneva Basin the study of the Carbon and Sulphur isotopes as well as the noble gases, hydrocarbon content will contribute reducing the uncertainty of the interpretation and providing new insights for future geothermal developments in the area.

4.7 Hydrochemistry monitoring at GEo-01

Since the execution of drilling operation, the hydrochemical composition of the fluid discharged by GEo-01 has been monitored to assess its possible evolution. As the pdocution tests are still running, final data and results will be available only after the end of the project and will be published in peer-review scienfitic journals.
If looking at the main major elements defining the geochemical facies of the GEo-01 groundwater, only minor fluctuations can be observed indicating stable hydrogeological conditions controlling the water-rock interactions. This is also supported by the high flow-rate and stable pressure conditions observed at the wellhead (see also Section 0).

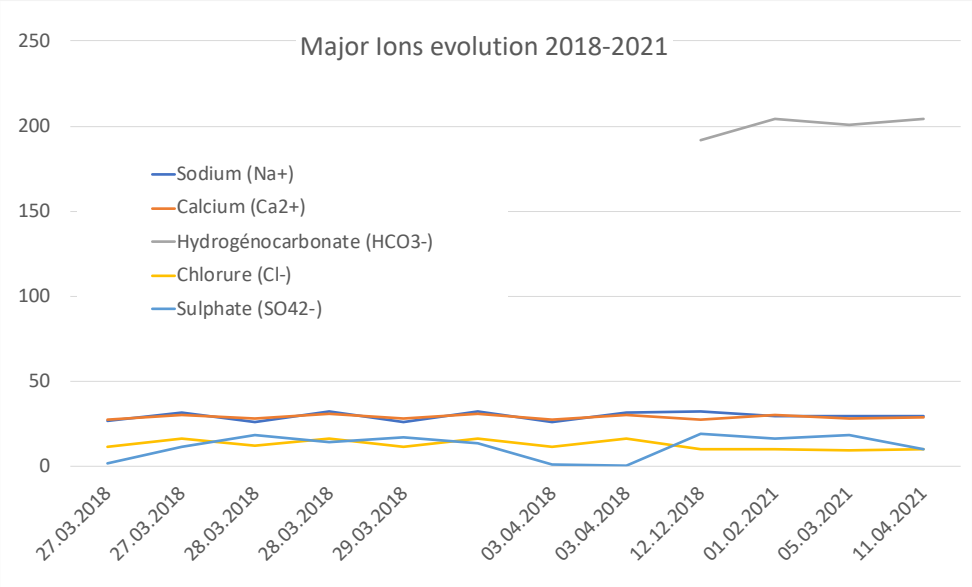

4.8 GEo-02 hydro-chemical features

In October 2020, SIG collaborated with IFP Energies Nouvelles and SEMM Logging to carry out a water sampling survey at depth at GEo-02 well. As no final report is available from IFP at the moment, this chapter reports only the results of the analysis with very little interpretation.
The schematic structure of the GEo-02 well is shown in Figure 15.

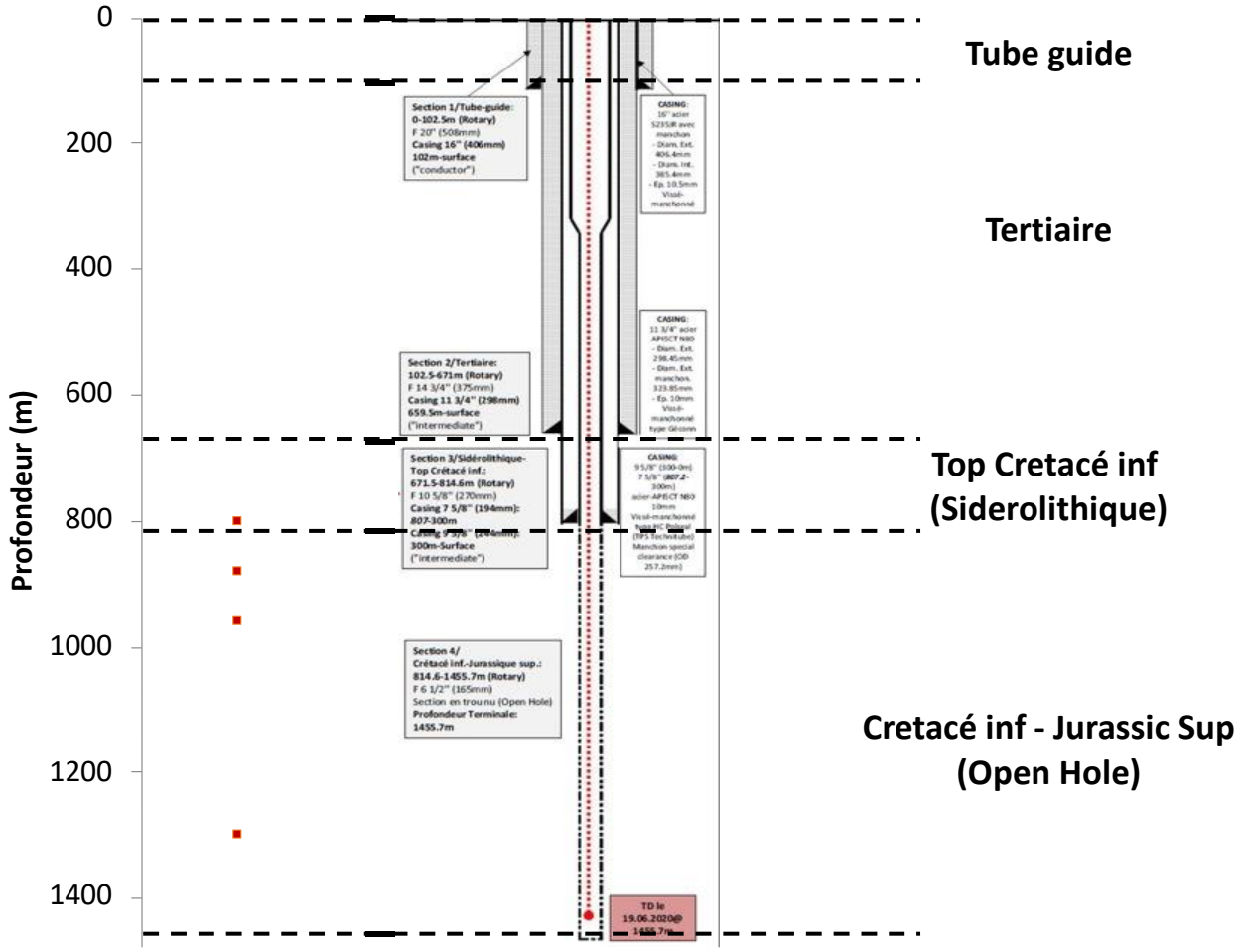

Figure 15. Structure of the GEo-02 well. The red dots indicated the sampling depths.

In total 2 surface (Table 9) samples and 5 sampling levels were collected in the Lower Cretaceous between 800 and 1361m in depth, focusing specifically on gas composition at the conditions resumed in Table 10. Table 11 reveals a very low contamination from atmospheric air, less than about 3.5%

Table 9. Surface water sampling and dissolved gas analysis for the samples collected at GEo-02.

	pH	Temperature (˚C)	Average CH4 (mmol/l)	Average $\partial^{13}C$ CH4 (‰)	Average DIC (mmol/l)	Average $\partial^{13}C$ DIC (‰)
Sample 13/10	8.14	16.4	0.43	-62.24	5.8	-1.5
Sample 15/10	8.31	11.2				

Table 10. Groundwater samples collected at GEo-02.

	Depth (m b.g.l.)	Fluid Volume (cc)	Temperature (˚C)	Pressure (bars)
Level 1 13/10	1360	570	51.0	133
Level 2 14/10	880	570	39	90
Level 3 14/10	996	570	42	101.5
Level 4 15/10	880	570	39.1	89.7
Level 5 15/10	800	570	37.5	82.3

Table 11. Results of the gas field analyses at GEo-02.

Sample	2 analyses	He	H2	O_2	N_2	Ar	CH_4	CO_2	C_2H_6	C_3H_8	H_2S	Total	% air
1360 m* 13/10	GWR=0.0003	0.02	0	0	99.2	0.14	0.27	0.36	0	0	n.a.	100	0.65
880 m 14/10	Average	0,08	0,0015	0	38,7	0,92	59,7	0,62	0,016	0,001	0,024	100,000	3,50
880 m 15/10	Average	0,07	0,0040	0	39,3	0,87	59,1	0,60	0,016	0,002	0,006	100,000	3,37
800 m 15/10	Average	0,06	0,0103	0	39,1	0,92	59,3	0,55	0,016	0,001	0,005	100,000	1,47

Table 12. Dissolved gas composition at well sampling conditions calculated with the SØreide Witson Thermodynamic Model at GEo-02.

Depth (m b.g.l.)	T (˚C)	P (bars)	CO_2 (mmol/l)	H_2S (mmol/l)	CH_4 (mmol/l)	C_2H_6 (mmol/l)	C_3H_8 (mmol/l)	N_2 (mmol/l)	H_2 (mmol/l)	He (mmol/l)	Ar (mmol/l)
880 13/10	39	90	0,29	1,32E-02	3,1	6,88E-04	2,87E-06	0,33	3,90E-05	0,007	0,11
880 15/10	39,1	89,7	0,29	3,40E-03	3,1	7,10E-04	8,34E-06	0,34	1,05E-04	0,006	0,10
800 15/10	37,5	81,5	0,36	3,62E-03	35,8	9,57E-03	5,22E-04	21,92	6,04E-03	0,034	0,56

Table 13. Results of the methane gas field analyses at GEo-02.

Depth (m b.g.l.)	$\delta^{13}C$ CH_4 (‰)	δD CH4 (‰)
880 m	-62,93	-242,0
800 m	-62,04	-249,1

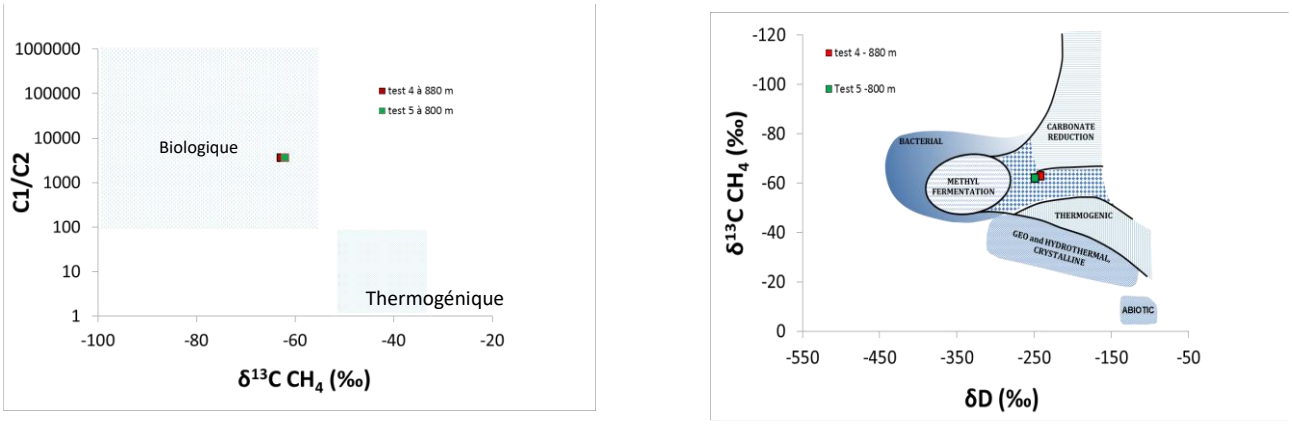

Figure 16. origin of Methan in the GEo-02 gas (Source: SIG/IFPN; plots modified after Whiticar et al., 1999).

Preliminary interpretation about the origin of CH_4 indicate that it derived from biogenic processes, mainly related to carbonate reduction and methyl fermentation.

5 Geophysical monitoring of the Satigny Geo-01 site (Geneva, Switzerland). Combined use of GPS, InSAR, seismometers and inclinometers for ground deformation assessment

This study was carried out to assess the potential of combined application of GPS, InSAR, seismometers and inclinometers to:

- Monitor the baseline deformation near and at the Geo-01 Satigny borehole before the production tests and its evolution during and after the tests
- Measure the troposphere state in the area using GPS
- Constrain surface deformation parameters and compare them to Thermo-Mechanic reservoir response stimulation as performed in Task 6.6

5.1 Methodology: GPS, InSAR and inclinometry in Satigny; high-grade collocated monitoring site in Switzerland.

The Satigny site is one of the best-equipped in the world. Because of the colocation (<1km) of one broadband seismometer, 2 permanent GPS and 2 inclinometers, plus the monitoring of the water parameters coming out of the borehole it allows innovative investigation impossible elsewhere.

The monitoring strategy is composed of three layers: GPS/InSAR, seismometer/inclinometers and water quality. These three layers allows to monitor vibrations (seismometer and inclinometers), long-term motions and tilts (GPS, InSAR and inclinometers) and at last atmospheric contributions (InSAR and GPS). Available space allowed temporary deployment of additional instruments (gravimeter of U of Neuchatel) for short periods.

5.1.1 GPS

With an inter-site spacing larger than 20-50 km, permanent GPS networks aim at describing continental scale deformation. Such design has been applied to build many Global Navigation Satellite systems (GNSS) networks including Plate Boundary Observatory (PBO), Pacific Northwest Geodetic Array (PANGA, Washington state), Bay Area regional Deformation (BARD, North California), EUropean REference Frame (EUREF) networks or GEONET in Japan and New Zealand. Denser permanent networks have been deployed (SCIGN in southern California in Los Angeles, GEONET New Zealand and miniPBO in Parkfield). Using permanent site data, and more than 15 years of survey, uncertainties on velocities are of the order of 0.4 +/- 3 mm/yr for both horizontal components and 1 mm/yr for the vertical one. The minimum detectable horizontal strain rate is ~10 nanostrain/yr.

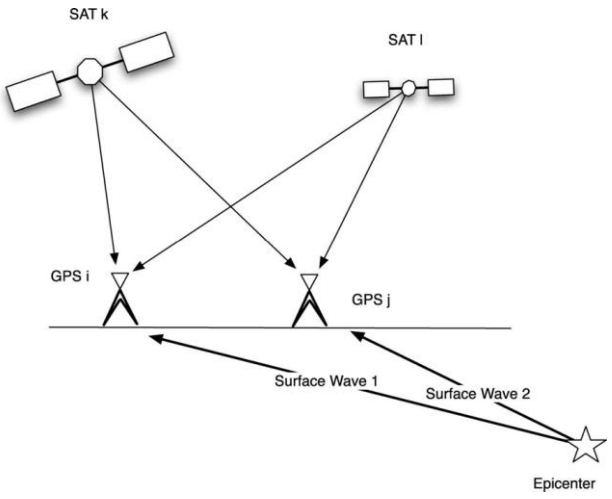

Figure 17. Schematic illustration of the ground shaking propagating along the surface and perturbing four radio ray-paths arriving at the two GPS sites i and j. The four residuals of the four signals received at site i and j are computed using GAMIT (King and Bock 2011). Because Rayleigh waves are not arriving at the same time to both sites, the residuals of the Double Difference are not equal to zero. Figure from (Houlié et al. 2011).

The question of what GPS measures is fundamental when we compare strain rates computed from GPS data with other datasets, or when we use GPS to characterize the level of activity of a fault or an area. The uncertainties mentioned above allow GPS networks to detect many types of processes involved in deforming the surface.
It is important to keep in mind that GPS essentially measures distances, not strain rates. Strain rates are obtained from the comparison of relative position of neighboring sites through time. The wavelength of the GPS strain rates directly depends on the spacing between sites. Continuous GPS (C-GPS) networks are usually not dense enough to detect interseismic and coseismic deformation related to small fault systems (L < 10km long) corresponding to M6.0 (or less) earthquakes (Wells and Coppersmith 1994). C-GPS networks are however well designed to constrain lithosphere deformation or even mantle deformation if the network is wide enough.
At Satigny, the motions detected by the two GPSs could be of tectonic origin but as the site may not be mature enough such motion signals may be found impossible to detect yet (Houlié and Stern 2017). Today, GPS may help detect the atmospheric noise, stabilize the local and regional network and at last detect the local motion induced by landslides (if any) and aquifer changes of state.

5.1.2 InSAR

As said above, vertical motions could not be as well detected as horizontal motions by GPS. For this reason, we have supplemented the monitoring by InSAR monitoring. Radar data are provided for free by European Space Agency (ESA) through the sentinel-1 mission (Attema et al. 2010 ; De Zan and Guarnieri 2006). This technique is tracking the topographic changes between two dates. The results of an InSAR computation is called an interferometer, which is an image made of 40m pixels, covering an area of about 50 x 50 km. The accuracy each pixel is close to 2.8mm. As for other very techniques, the signal include contributions which are not targeted in the first place by the technique such as atmospheric changes, road works, farming activities. The containment of very local noise pollutions rely on the differential analysis of the signals.

For atmospheric noise, solutions exists. As for GPS it is well known that InSAR is well sensitive to atmospheric noise. However the combination of both techniques with meteorological data could be used in order to improve the quality of the InSAR imagery and of GPS time-series (Houlié et al. 2016).

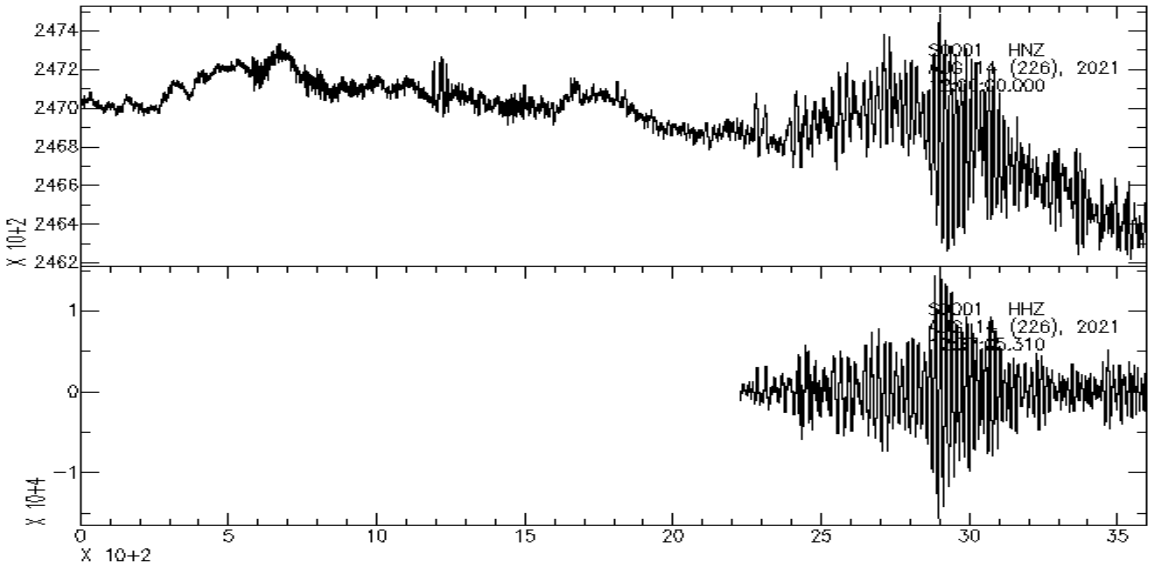

Figure 18. Data collected during the seismic wave propagation of the Haiti earthquake (2021-08-24).

5.1.3 Inclinometry / Seismology

At last, we support the poor spatial resolution of GPS (one point per km or less measured every 15s) and of InSAR (40m pixel very 11 days or more) by adding a high-resolution temporal records by deploying two inclinometers to improve the monitoring already in place and based mostly by the SIG seismometer located in Satigny. Those instruments are recording data at 20Hz. One is located at the Geo-01 borehole and another in the hills above (Figure 6).The inclinometer recorded high quality data including the seismic waves propagation of the Haiti 2021 earthquake.

5.2 Data collection

5.2.1 Installation of two GPS sites (Geo-01 and Satigny-01)

Instrumentation context. Before the start of this project, the GPS coverage in the area of Geneva was poor (one site within > 20 km located at the CERN). Since the archiving of the Service Industriels de Genève (SIG) and of Direction de l'information du territoire - Etat de Genève GPS sites (DMO2 and DCMO) plus the addition of the two sites in the framework of the current project (SAT1 and SAT2), we now can use 5 GPS sites in the Geneva area. These GPS sites are still not mature (less than 5 yrs of data collected) but they will complement the existing permanent GPS network located in the European platform and within the Alpine arc. About maturity of GPS instrumentation, please refer to Figure 3 of Houlié and Stern (2017).

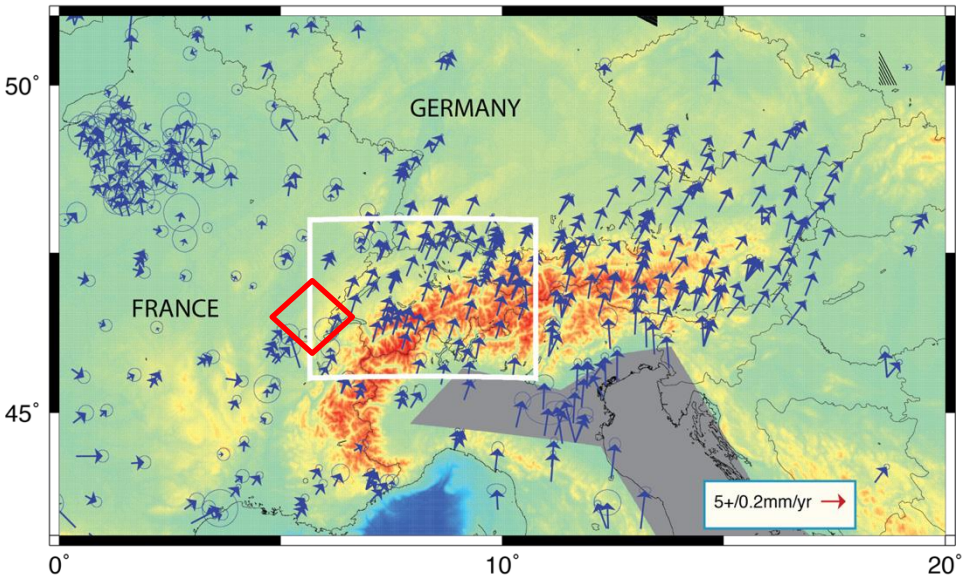

Figure 19. GPS network used in this study. Solutions previously computed were compared with newly added data. It is obvious that the permanent GPS network in west Switzerland lies on French and Italian networks for stability. The area of interest is located using a red diamond. Figure from (Houlié et al. 2018).

Tectonic context, nature of the surface deformation. From the recent research in the area, beyond slow surface deformation which is linked to the relative motion of geological units between Alpine and Jura chains, we only expect only moderate deformation mostly composed of horizontal shear strain. As the seismicity level is low to moderate, we expect that if deformation is observed, it may be linked either to human activities (geothermal, aquifer pumping, tunnel drilling, etc.) or to natural causes such as aquifer recharge, tectonic loading).

SAT1 and SAT2 GPS sites. Two Trimble units were installed on steel pipes by Nicolas Houlie Geologie GmbH, Zurich (http://www.nicolashoulie.com). At the Geo-01 site, the antenna was installed into the concrete structure (Figure 2). The other GPS antenna has been attached to a small storage building as no local bedrock was available. This second site was used to stabilize the troposphere model during the processing of the data. The antennas used at SAT1 and SAT2 are of Trimble Zephyr Geodetics.

Both GPS sites are co-located with inclinometers (ROCTEST brand). The sites were fully operational at the fall 2020, two months before the start of the production test (23 December 2020). Telemetry was installed at the two sites in order to collect and transmit data at an hourly rate using Teltonika modems and Centaur dataloggers. Data were then stored on a remote-server and backed up at Nicolas Houlie Geologie GmbH. Seismic data collected at Satigny are following the same telemetry path.

a)

b)

Figure 20. Photos of the GPS antenna (SAT2) at the Geo-01 site (a) and photo of the ROCTEST Inclinometer collocate to the SAT1 GPS antenna (b).

5.3 Results

5.3.1 GPS time-series

All data were collected at 15s and then subsampled for processing at 30 seconds. The GPS data processing was defined following guidelines as defined in (Houlié and Romanowicz 2011; Houlié et al. 2018). The solutions obtained during previous research projects were compared to current solutions in order to assess the quality of the data. The processing was including existing positions in the ITRF 2008 (International Terrestrial Reference Frame; Altamimi et al. (2012)). We show in Figure 2, the permanent GPS sites which were available for processing in the area. Some of them are part of the ITRF2008 such as ZIMM, ZIM2 and BSCN (Besancon, France).

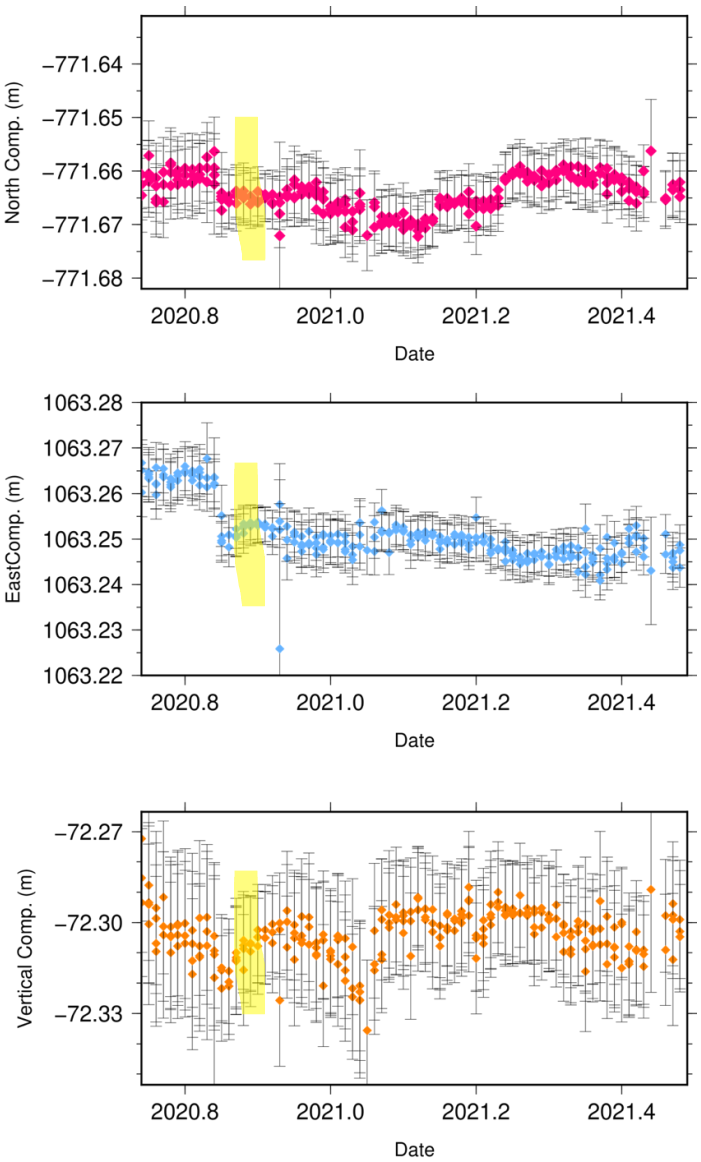

Figure 21. SAT1-SAT2 baseline components from mid-2020 to mid-2021. Components are computed using the formula SAT2-SAT1. We show the start of the productions tests by using a yellow rectangle. The time-series presented here are used to constrain the Young modulus of the reservoir (Deliverable 6.6; Figure 41).

We show in Figure 3 the baseline parameters between the sites SAT2 (Geo-01) and the site located at the SAT1 (located in the wine country close to the locality of Choully. Those show that since December 2020 no motion could be detected using data collected GPS located at SAT1 and SAT1 over the production testing period. It suggests no deformation has been occurring during the production phase.

5.3.2 Sentinel1 (InSAR)

Nicolas Houlie Geology GmbH processed > 360 interferograms covering the period May 2020 to May 2021. All data used are Copernicus **Sentinel data** [2020, 2021]. Retrieved from ESA [06 06 2021], processed by ESA.All data were processed using GMT/GMTSAR tool Suite. Data are visualized using the software QGIS (QGIS Development Team 2009). The coverage obtained from the processing is good with a very good coverage of the Satigny.

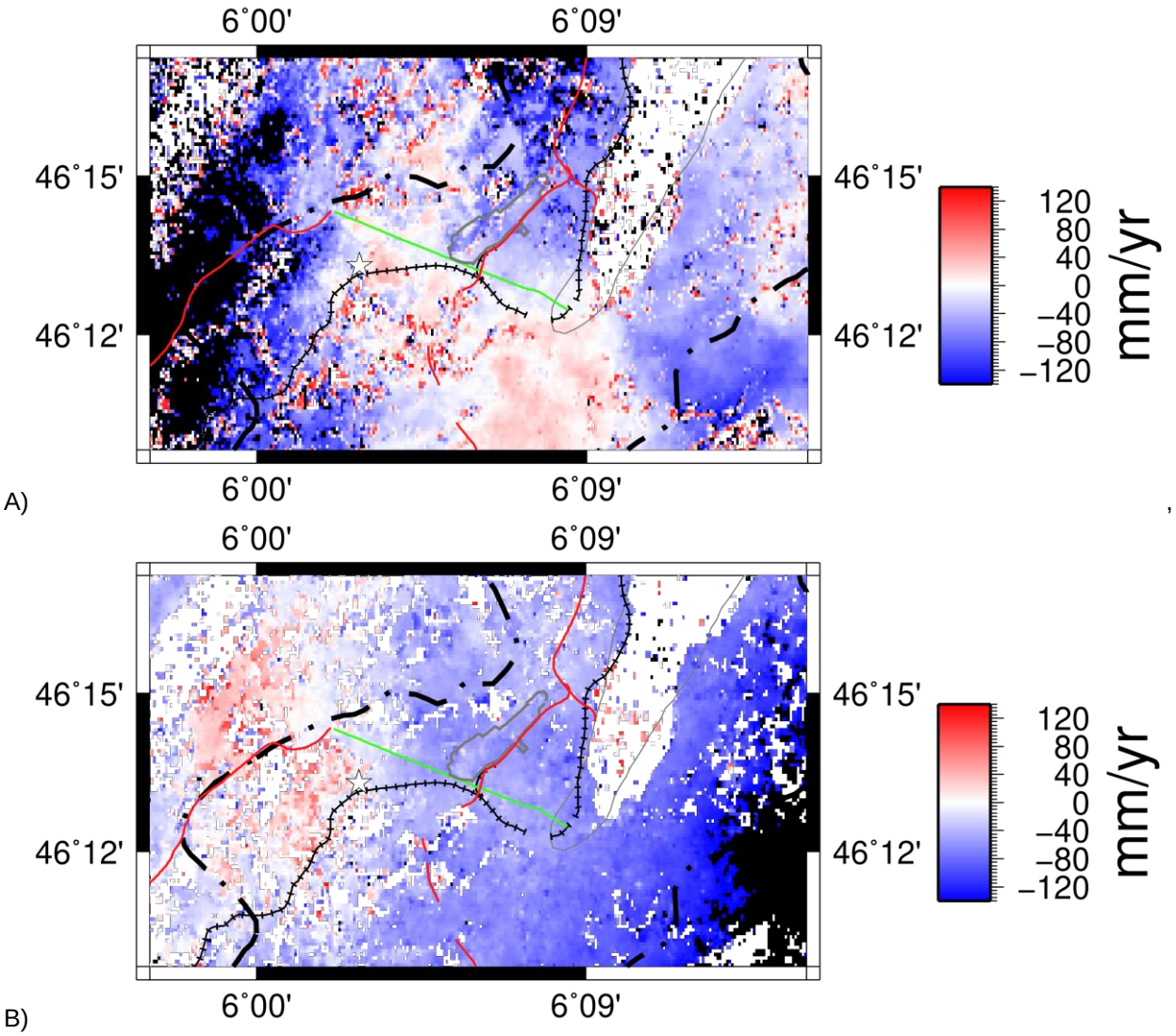

Figure 22. Average surface motion (mm/yr) between A) December 2020 and Jan 2021 and B) October 2020 in the surrounding of the GEO-1 site (white star). For the purpose of location , we locate main train lines with faulted black lines, highways using red lines. The Route de Meyrin is shown as a green line, the footprint of the airport in grey.

As expected, atmospheric noise is contributing to most of the signal for interferometers made in for Geneva area. This is not problematic as local features can still be constrained through the analysis of the motion horizontal gradient (Figure 7). Some geological features are visible on some images (Figure 8), mostly for images covering wet-dry transition periods. For instance, the motion along the shoreline of the Geneva lake (blue square) and near the Golf (white square). In 2021, we can note for the future that the period was quite humid in Switzerland; drought effects may appear in the coming months. Troposphere corrections may be necessary to improve the image quality.

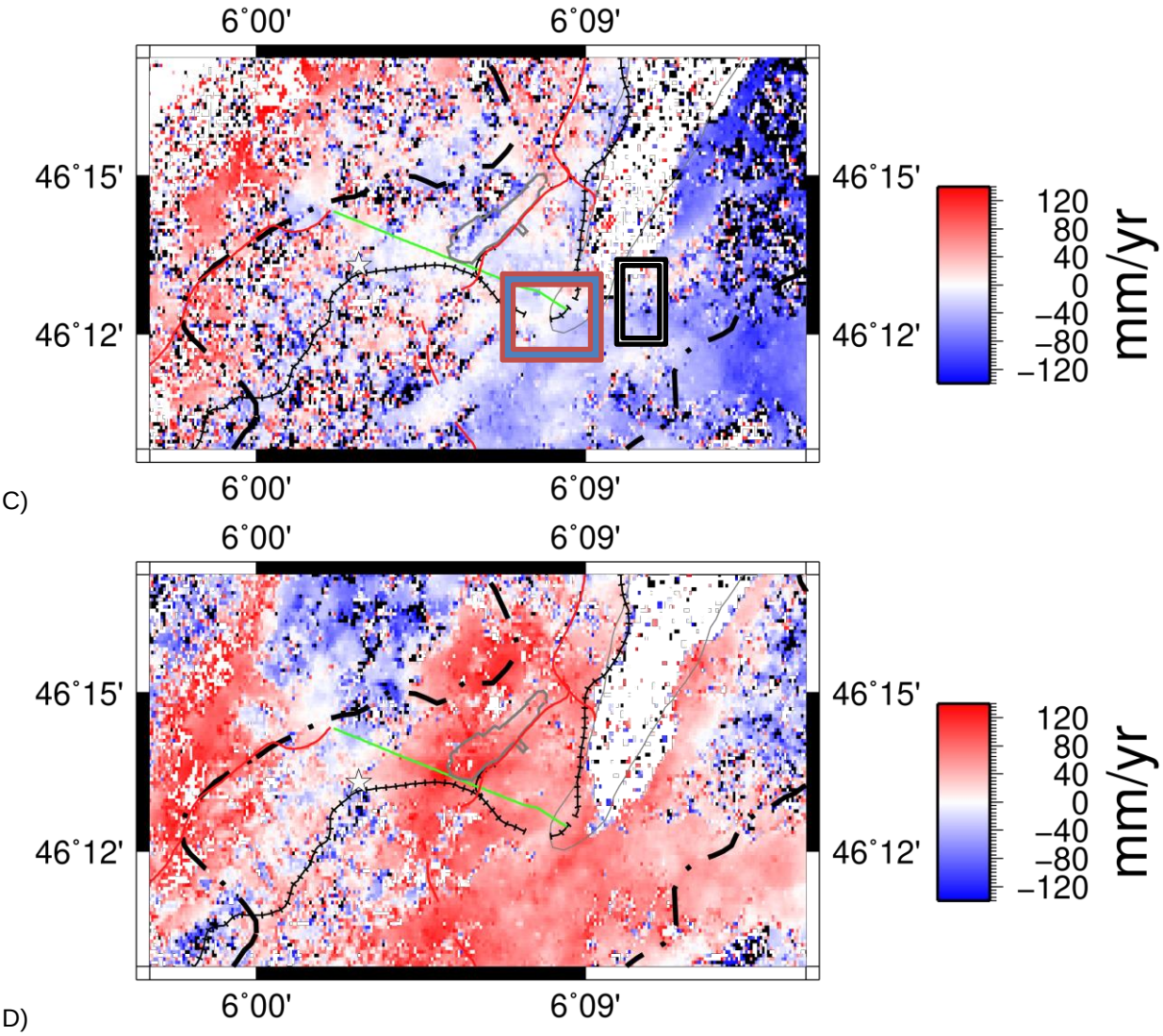

Figure 23. continued, C) April 2021 and D) March 2021 in the surrounding of the GEO-1 site (white star). For the purpose of location , we locate main train lines with faulted black lines, highways using red lines. The Route de Meyrin is shown as a green line, the footprint of the airport in grey.

5.4 Conclusions and Perspectives

We would have needed more observation time from the GPS, but we have been limited in time because of COVID-19 pandemia (missing parts due to border closed, access to site impossible, installation delayed, etc.) which reduced the observation time by a couple of months). The GPS observation is planned to continue up to December 2021. Data currently collected will be analyzed to reach some conclusions in an academic report. For instance, more analysis will be carried through the atmospheric characterization during the preparation of a research article (Birdsell et al., 202X) focusing on the properties of the reservoir parameters. This analysis will be following the guidelines defined by (Houlié et al. 2016).

The monitoring of the reservoir has been started month before the start of the current project. The reanalysis of the InSAR data collected during the period preceding the production test will allow defining a clear baseline of the area of Satigny.

The Satigny site located at the Geo-01 site is indeed one of the few sites in the world where instrumentation of various types are collocated (Psimoulis et al. 2014). Here we are able to compare data collected by inclinometers, seismometers and GPS data. The continuation of this experiment will allow assess data quality and to make progresses in instrumentation (testing, calibration, etc.). Inclinometry will allow the description of very low amplitude motions which are not detected by seismometers (signal too slow to develop) or by GPS (amplitude threshold much higher).

5.5 Next steps

- During the end of the project (funded by SIG and planned for December 2021), InSAR time-series will be built and atmospheric noise will be compared with meteorological data for some selected periods. This will allow a finer analysis of the InSAR data and a consistent analysis of the GPS data.
- The data collected during the Haiti 2021 earthquake (Figure 4) will allow the establishment of a better instrument response than the response delivered by the hardware provider.
- GPS data are today still collected and it is up to SIG to continue (or not) the GPS monitoring at these two sites.

6 References

Altamimi Z, Métivier L, Collilieux X (2012) ITRF2008 plate motion model. J Geophys Res 117(B7).

Attema E, Cafforio C, Gottwald M, Guccione P, Monti Guarnieri A, Rocca F (2010) Flexible dynamic block adaptive quantization for Sentinel-1 SAR missions. IEEE Geoscience and Remote Sensing Letters 7(4):766-770.

Clerc M. and Moscafiello A. (2020). A revised structural framework for the Geneva Basin and the neighbouring France region as revealed from 2D seismic data: implications for geothermal exploration. Swiss Bull. angew. Geol.

De Zan F, Guarnieri AM (2006) TOPSAR: Terrain Observation by Progressive Scans. Geoscience and Remote Sensing, IEEE Transactions on 44(9).

Eruteya O, Guglielmetti L, Moscariello A (2021) 3D geologic model of the GEo-01 well area. . In: Project GECOS - Geothermal Energy Change of Success.

Guglielmetti L, Eichinger F, Moscariello A (2020) Geochemical Characterization of Geothermal Waters Circulation in Carbonatic Geothermal Reservoirs of the Geneva Basin (GB). In: World Geothermal Congress 2020. Reykjavik.

Houlié N, Funning G, Bürgmann R (2016) Use of a GPS-derived troposphere model to improve InSAR deformation estimates in the San Gabriel Valley, California. Trans. Geosc. Rem. Sensing 54(9):5365-5374.

Houlié N, Occhipinti G, Blanchard T, Shapiro N, Lognonne P, Murakami M (2011) New approach to detect seismic surface waves in 1Hz-sampled GPS time series. Sci Rep 1:44.

Houlié N, Romanowicz B (2011) Asymmetric deformation across the San Francisco Bay Area faults from GPS observations in Northern California. Phys. Earth Planet. Inter. 184(3-4):143-153.

Houlié N, Stern TA (2017) Vertical tectonics at an active continental margin. Earth Planet. Sc. Lett. 457:292-301.

Houlié N, Woessner J, Giardini D, Rothacher M (2018) Lithosphere strain rate and stress field orientations near the Alpine arc in Switzerland. Sci. Rep. (8).

King B, Bock Y (2011) GAMIT manual. In Psimoulis P, Houlié N, Michel C, Meindl M, Rothacher M (2014) Long-period surface motion of the multi-patch Mw9.0 Tohoku-Oki earthquake. Geophys J Int. 199:968-980.

QGIS Development Team (2009) QGIS Geographic Information System. In,

Services Inddustriels de Geneve (2020). Rapport de fin sondage GEo-01. Unpiblished report, pp. 137-170.

Services Inddustriels de Geneve (2020). Projet SECURE, echantillonage GEo-02. Presentation IFPN Energie Nouvelles.

Wells DL, Coppersmith KJ (1994) New empirical relationships among magnitude, rupture length, rupture width, rupture area, and surface displacement. Bulletin of Seismological Society of America 84:974-1002.